Genomic and structural features of the Yellow Fever virus from the 2016-2017 Brazilian outbreak

Mariela Martínez Gómez[1], Filipe Vieira Santos de Abreu[2,3], Alexandre Araujo Cunha dos Santos[1], Iasmim Silva de Mello[1], Marta Pereira Santos[1], Ieda Pereira Ribeiro[1], Anielly Ferreira-de-Brito[2], Rafaella Moraes de Miranda[2], Marcia Gonçalves de Castro[2], Mario Sergio Ribeiro[4], Roberto da Costa Laterrière Junior[5], Shirlei Ferreira Aguiar[6], Guilherme Louzada Silva Meira[6], Deborah Antunes[7], Pedro Henrique Monteiro Torres[7], Ana Carolina Paulo Vicente[8], Ana Carolina Ramos Guimarães[9], Ernesto Raul Caffarena[7], Gonzalo Bello[10], Ricardo Lourenço-de-Oliveira[2*], Myrna Cristina Bonaldo[1*]

1- Laboratório de Biologia Molecular de Flavivírus, Instituto Oswaldo Cruz, Fundação Oswaldo Cruz, Rio de Janeiro, Brazil.

2- Laboratório de Mosquitos Transmissores de Hematozoários, Instituto Oswaldo Cruz, Fundação Oswaldo Cruz, Rio de Janeiro, Brazil.

3- Instituto Federal do Norte de Minas Gerais, Salinas, MG, Brazil.

4- Superintendência de Vigilância Epidemiológica e Ambiental, Secretaria Estadual de Saúde, Rio de Janeiro, Brazil.

5- Núcleo Especial de Vigilância Ambiental, Secretaria Estadual de Saúde do Espírito Santo, Vitória, Brazil.

6- Laboratório Central de Saúde Pública Noel Nutels (LACEN-RJ), Rio de Janeiro, Brazil.

7- Programa de Computação Científica (PROCC), Fundação Oswaldo Cruz, Rio de Janeiro, Brazil.

8- Laboratório de Genética Molecular de Microorganismos, Instituto Oswaldo Cruz, Fundação Oswaldo Cruz, Rio de Janeiro, Brazil.

9- Laboratório de Genômica Funcional e Bioinformática, Instituto Oswaldo Cruz, Fundação Oswaldo Cruz, Rio de Janeiro, Brazil.

10- Laboratório de AIDS e Imunologia Molecular, Instituto Oswaldo Cruz, Fundação Oswaldo Cruz, Rio de Janeiro, Brazil.

***Corresponding author:**

Correspondence and requests for materials should be addressed to R.L.-d.-O. (email: lourenco@ioc.fiocruz) or M.C.B. (mbonaldo@ioc.fiocruz.br).

Keywords: Yellow fever virus, 2016-2017 Brazilian outbreak, amino acid changes, genetic diversity, evolution

48 **ABSTRACT**

49 Brazil has been suffering a severe sylvatic epidemic of yellow fever virus (YFV)
50 since late 2016. Analysis of full-length YFV genomes from all hosts involved in the
51 Brazilian 2017 outbreak reveals that they belong to sub-lineage 1E within modern-
52 lineage, but display several unique amino acid substitutions in highly conserved positions
53 at NS3 and NS5 viral proteins. Evolutionary analyses indicate that YFV carrying that set
54 of amino acid substitution circulates in the Southern Brazilian region for several months
55 before being detected in December 2016. Structural and selection analyses support that
56 some of these substitutions were under positive selection and could impact enzyme
57 structure and function. Altogether, this evidence demonstrated that the current Brazilian
58 YFV carries unique amino acid signatures in the non-structural proteins and support the
59 hypothesis that those substitutions may be affecting the viral fitness and transmissibility.
60

61 **INTRODUCTION**

62 Yellow fever (YF) is a viral disease transmitted by the bite of infected mosquitoes
63 in Africa and South America, affecting around 200,000 people annually, mostly in Africa
64 (1-3). There are two main epidemiological cycles: the enzootic sylvatic cycle where the
65 virus is transmitted between non-human primates (NHP) and wild arboreal mosquitoes of
66 genus *Aedes, Haemagogus* and *Sabethes*, and in which humans can be accidentally
67 infected, and the urban cycle where inter-human transmission is ensured by the domestic
68 and anthropophilic mosquito *Aedes aegypti* (3). While only the sylvatic cycle has been
69 reported in the Americas during nearly the last 75 years, in Africa people may acquire the
70 infection in both cycles, besides in an intermediate cycle occurring in rural areas close to
71 forests (2, 4).

The causative agent is the yellow fever virus (YFV) (genus: *Flavivirus*, family: *Flaviviridae*), presenting a single-positive-sense RNA genome, containing a 5' end cap structure, that is translated in a single immature polyprotein precursor. The precursor polyprotein is cleaved into three structural proteins, capsid (C), envelope (E), and membrane protein (M) and seven non-structural proteins, NS1, NS2A, NS2B, NS3, NS4A NS4B, and NS5 (2). The virus was originated in Africa, where five genotypes have been documented, being two from West Africa (West Africa I and II) and three in East and Central Africa (East Africa, East/Central Africa, and Angola). The YFV virus has spread from Africa to the Americas together with the invasive mosquito *Ae. aegypti* where it evolved in the last four centuries into two genotypes (South America I and II) derived from the Western African ancestor (5-7). The South American genotype I is the most spread and frequently detected during the epizootics and epidemics waves in Brazil and other countries of South America (8, 9). Until the 1990's, the transmission area in Brazil was primarily limited to the Amazon forest, in the Northern, and the savanna-like *cerrado,* in Center-West region. However, in about two decades, the YFV territory has progressively expanded Southward and Eastward reaching the Atlantic forest and other biomes from the country´s most populated regions(10). During this boundary expansion, five viral sub-lineages (1A to 1E) successively arose within the genotype I. They were distinguished by analysis of partial nucleotide sequencing of the YFV genome particularly the pre-membrane and envelope (prM/E) gene junction (8, 9, 11). Most recently, South America genotype I was divided into two major lineages named as Old lineages (enclosing Old Para, and 1A, 1B, and 1C sub-lineages) and Modern lineage (enclosing Trinidad and Tobago, and 1D and 1E sub-lineages) (11, 12).

A rapid expansion of the YFV area has reported since late 2016 in Southeast Brazil (Fig.1) (13, 14). From December 2016 to May 2017, the YFV quickly spread from the

transition zone between the *cerrado* and the Atlantic forest inland of Minas Gerais State (MG) to the coastal areas in the Espírito Santo (ES) and Rio de Janeiro (RJ) states, then approaching to densely populated sites with insignificant vaccination coverage under influence of the rain forest. A YFV outbreak of unprecedented sanitary severity and causing an ecological disaster was recorded. In a few months, around 3,850 NHPs died, and nearly 800 human cases with 435 deaths were registered, of which 274 were YF confirmed until July 2017 (13, 14). Interestingly, during this ongoing outbreak analysis of complete nucleotide genome sequences of the YFV obtained from the blood of two howler monkeys from a single locality in ES confirmed that they cluster within the sub-lineage 1E. Furthermore, these strains revealed new polymorphisms comprising several amino acid substitutions mainly located in the components of the viral replicase complex, in the protease domain of the NS3 protein, and in the methyltransferase (MTase) and RNA-dependent RNA polymerase (RdRp) domain of the NS5 protein(15). The NS3 protein, a viral multi-functional protein, carries a chymotrypsin-like serine protease activity (NS3pro) at its N-terminal and an helicase activity (NS3hel) at its C-terminal domain(16). The NS3pro associated with its cofactor NS2B cleaves all cytoplasmic protein junction sites of the precursor polyprotein. The NS5 protein contains two functional domains with a capping related MTase and the central replication enzyme RdRp (17-19). Connecting MTase and RdRp, there is a linker of 5–6 residues (residues 266–271; NS5 Dengue virus position), which has an essential role in NS5 conformation and protein activity (20). Also, NS3 and NS5 have been associated with innate immune system evasion (21, 22). It was unclear, however, whether the observed amino acid substitutions are genetic signatures of the most recent YF outbreaks as few complete genomes of current circulating viral strains were available (8, 15).

In this study, we elucidated the complete genome sequence of 12 YFV strains from three hosts (NHPs, mosquitoes, and humans) involved in the transmission cycle of the current Brazilian outbreak in two Southeastern states (RJ and ES). Sequences were analyzed to establish whether specific amino acid changes previously observed are fixed in other recent YFV samples and therefore constitute a molecular signature of the 2017 YFV. We also created homology models for NS3 and NS5 to determine the location and potential effects of amino acid substitutions on NS3pro and NS5 proteins. Moreover, we performed phylogenetic and evolutionary studies to analyze the codons that might be under positive selection pressure and to estimate the time of the most recent common ancestor (T_{MRCA}) of Brazilian YFV 2017 samples.

RESULTS

YFV samples geographic distribution and genome characterization

From February to June 2017, we collected 15 YFV samples from five distinct infected host species including mosquitoes, NHP and humans from 11 localities belonging to three main river basins across the current epidemic/epizootic territory in the Atlantic coast in ES and RJ (Table 1; Fig. 1). We determined and analyzed the whole YFV genome of twelve samples: two pools of infected mosquitoes belonging to two species *Haemagogus leucocelaenus* and *Hg. janthinomys*, six from NHP (four howler monkeys and two marmosets), and four from human cases (Table 1). Partial sequences of the YFV genome were also obtained from an additional human case (H189) (data not shown).

The comparison of all the YFV genomes from the ongoing Southeast Brazilian outbreak reveals low genetic variation, providing a mean nucleotide identity of 99.8 % and amino acid identity values ranged from 99.9% to 100%. However, part of the

nucleotide variations is non-synonymous, leading to new amino acid substitutions in the polyprotein sequence (Fig. 2; Supplementary file 1). Regardless the host, all the 2017 YFV Brazilian genomes display a set of eight unique amino acid substitutions, that we have recently identified in two YFV samples from infected howler monkeys (ES-504 and ES-505) from ES state (15). Remarkably, the comparison with the genome of other South America strains confirmed that these polymorphisms are only present in the Brazilian strains from the ongoing outbreak when comparing with other South American strains. They localize at C protein (V108I), at NS3pro (E1572D; R1605K), at NS5 in MTase domain (K2607R; V2644I; G2679S), and at NS5 in RdRp domain (V3149A; N3215S) (Fig. 2). Nevertheless, the partial nucleotide sequence from H189 also displayed all amino acid changes detected in the other sequences, except for the mutation in the C protein. Moreover, all 2017 YFV Brazilian strains also share an amino acid change at position N/D2803S that was previously observed only in a Venezuelan strain isolated in 2006 (GenBank, KM388818). We also detected additional amino acid substitutions, which are not present in all the 2017 Brazilian genomes (Fig. 2). Accordingly, the YFV H199 sequence shows a change from an alanine (A) to a serine (S) at the amino acid position 826, corresponding to the NS1 protein (position 48). The YFV genomes RJ95, RJ96, RJ97, H191 and PA193, show a substitution from an isoleucine (I) to a valine (V) at position 2176 (NS4A, position 77). The phylogenetic analysis of prM/E sequences indicates that all 2017 YFV Brazilian strains cluster inside sub-lineage 1E of the Modern lineage of South America genotype I in a monophyletic clade with high support (bootstrap = 87 %) (Fig. 2 – Fig. Supplement 1). The same clustering pattern was obtained when we performed the phylogenetic analyses of either NS3 or NS5 nucleotide sequences (Fig. 2 – Fig. Supplement 2).

Modeling and Structural Analysis of NS2B/NS3 and NS5 proteins

We created structural models of NS3 and NS5 proteins to gain some insights into the structural and functional effects of these amino acid substitutions. Initially, prior to the structural model generation, we aligned the NS3 and NS5 amino acid sequences of the prototype 2017 Brazilian YF virus (strain ES505) (15) with the different template sequences (Fig. 3– Fig. Supplements 1; Fig. 4– Fig. Supplements 1).

The effect of the amino acid substitutions on both NS3 and NS5 proteins was evaluated through hydrogen bond formation and electrostatic analysis. The two substitutions found in NS3, E88D and R121K (polyprotein position: E1572D; R1605K, respectively) are conservative and, as such, they have little impact on the surface electrostatic potential (Fig. 3 C, D). For the E88D substitution, a small structural change was observed, which mainly consisted of lysine 174 (polyprotein position: K1658) side chain displacement due to the loss of a hydrogen bond with the protein backbone (Fig. 3 E, F). On the other hand, the R121K substitution is located near the NS2B binding groove and might influence the interaction between these two molecules. Hydrogen bond analysis indicates that K 121 could favor the formation of a hydrogen bond with threonine 77 of NS2B (polyprotein position: T1431), whereas such an interaction was not identified in 2010 model (Fig. 3 A, B). This interaction could, in turn, modulate the NS3-NS2B binding affinity and, thus, the protease efficiency.

The three first amino acid substitutions in NS5 are clustered in the MTase domain, whereas the remaining ones are in the RdRp domain. All amino acid substitutions at the MTase domain are conservative, but they are spatially adjacent. Arginine 101 (polyprotein position: R2607) alpha carbon is 9.7 Å away from that of isoleucine 138 (polyprotein position: I2644), which in turn is 10.6 Å away from serine 173 alpha carbon (polyprotein position: S2679). These three residues face the RdRp domain tunnel opening (Fig. 4B), which presents a basic electrostatic profile to accommodate the YFV RNA

196 molecule (Fig. 4 – Fig. Supplement 2), suggesting that they may influence the enzyme
197 activity.

198 Additionally, the N297S substitution (polyprotein position: N/D/S 2803) from the
199 RdRp domain, although being conservative, is located near the hinge domain. The
200 remaining two amino acid alterations: V643A (polyprotein position: V/A 3149) and
201 N709S (polyprotein position: N/S 3215) are located at the protein surface and are also
202 conservative. The combined effect of the mutations on the NS5 protein dynamics was
203 assessed through molecular dynamics simulations, which indicate that the NS5 protein
204 from 2017 sample has a decrease in fluctuation around the hinge region (Fig. 4– Fig.
205 Supplement 3).

206 **Selection analyses**

207 The mean dN/dS ratio of substitutions per site estimated by the SLAC method for
208 the South America genotype I (SAI) and West Africa (WA) data sets was 0.05 and 0.04,
209 respectively; thus indicating that purifying selection was the main evolutionary force of
210 both YFV genotypes. Tests for negative/positive selection, however, reveal some
211 important differences in the evolutionary dynamics of both genotypes (Fig. 5).

212 Selection analysis of the SAI dataset identifies 13 codons with evidence of
213 positive selection, including nine sites with evidence of episodic diversifying selection
214 (MEME), four sites with evidence of pervasive diversifying selection (FEL and/or
215 FUBAR) and one site identified by all three algorithms (FEL, MEME, and FUBAR).
216 Most sites (69%, 9/13) under positive selection were concentrated in a short genome
217 segment (2,100-2,850 codon positions) coding for non-structural proteins NS4A
218 (I2176V), NS4B (H2311L, N2408S, K2502N, T2503I) and NS5 (R2601K, R2640P,
219 D2647V, N/D2803S) (Fig. 5 – Fig. Supplement 1). Selection analysis of the WA dataset,
220 by contrast, detected no sites under pervasive diversifying selection and identified 18 sites

with evidence of episodic diversifying selection (MEME) uniformly distributed along structural and non-structural proteins (Fig. 5 – Fig. Supplement 1).

Evolutionary analyses

The Bayesian MCC tree inferred from the complete coding sequence (CDS) of YFV South American genotypes I and II reveals that YFV strains from the ongoing Southeast Brazilian outbreak grouped in a highly supported (*Posterior Probability* [*PP*] = 1) monophyletic cluster nested within sub-lineage E strains of the modern-lineage (Fig. 6). We further observed that 2017 YFV Brazilian strains segregate in two reciprocally monophyletic subgroups, one sub-cluster comprising strains of mosquitoes, NHP and humans from RJ and ES states (sub-clade A) (*PP* = 0.29), and one highly supported (*PP* = 0.99) sub-cluster containing YFV strains of NHP and humans from the state of RJ (sub-clade B). The median substitution rate of YFV South American genotypes complete genomes was estimated at 3.5 x 10^{-4} subst./site/year (95% HPD: 2.4-4.8 x 10^{-4} subst./site/year), in agreement with previous estimations(12). The median T_{MRCA} for all Brazilian 2017 YFV strains was estimated in April 2016 (95% HPD: July 2015 - October 2016) and for the sub-clade B at October 2016 (95% HPD: April 2016 - January 2017). In addition, the median T_{MRCA} of Venezuelan and Brazilian 2017 YFV strains was estimated as occurred 24 years ago.

DISCUSSION

In the 2016-2017 YFV outbreak in Southeast Brazil, most of the epizootics and human cases originally occurred in inland rural areas of MG and subsequently in Eastern Atlantic coastal sites under the influence of the ES rain forest segments. After that, the YFV spreading approached and even touched the Great Metropolitan areas of Vitoria (ES) and Rio de Janeiro (RJ), where lived nearly 1.8 and 12.3 million unvaccinated

246 inhabitants, respectively. Alarmingly, these densely populated areas host some of the
247 busiest South American airports, ports and road networks, are highly infested by YFV
248 competent urban vectors, *Aedes aegypti* and *Ae.albopictus,* and have repeatedly been the
249 territory of severe dengue epidemics. All together, these ecological and sanitary marks
250 raised concern about the potential risk of YFV to reemerge in an urban cycle in Brazil as
251 well as to spread to other countries and continents rapidly(23, 24). Furthermore, YFV
252 strains characterized by a set of amino acid polymorphism were identified during this
253 outbreak, and their biological impact needed to be investigated (15).

254 Regardless of deriving from five distinct host species infected in a six month lag
255 in 11 sites dispersed along 350 Km of the Southeast Brazilian coast across the outbreak
256 territory including the Great Metropolitan area of Rio de Janeiro, the YFV samples
257 analyzed in the current study are almost identical at the nucleotide and amino acid levels.
258 Also, they share a molecular signature represented by nine amino acids, being eight in
259 highly conserved positions at NS3 and NS5 encoding regions, and one in the structural
260 capsid protein. Previous analysis of 2017 YFV from two howler monkeys from a single
261 site in ES had not considered the substitution at position 2803 at NS5. However, in the
262 current study, the analysis of a higher number of samples allowed the identification of
263 one more substitution at position 2803 at NS5 in all 2017 YFV. This molecular signature
264 represented by nine amino acids have never been observed before in South-American and
265 African genotypes (15).

266 Hypothetically, amino acid changes at conserved protein positions of NS3 and
267 NS5 may have a role in the capacity of viral infection to vertebrate and invertebrate hosts
268 and thus accelerating the spreading of the ongoing outbreak. The NS3 and NS5 proteins
269 have multiple enzymatic activities essential for viral RNA replication and 5´-capping (25-
270 27). For these reasons, we also investigated the impact of the identified amino acid

substitutions through the structural analysis of NS3 and NS5 protein models. Even though all the amino acid substitutions were mainly conservative, they occur close to domains that might be affected by these subtle modifications. Furthermore, we were able to detect features that may correlate with an increase in enzymatic efficiency and constitute an advantage in viral dissemination. In the NS3 protein, the R121K substitution is located in the region responsible for the interaction with NS2B, the cofactor for the proteolytic activity of this enzyme. Although both residues bear a positive charge, lysine was shown to potentially establish a hydrogen bond with NS2B, due to the less bulky side chain. For the NS5 protein, we found that the three amino acid substitutions located at the MTase domain were spatially contiguous and could influence the relative orientation between the two domains. The N297S substitution might also have a significant role in the enzymatic efficiency since is located near the hinge domain. Hence, molecular dynamics simulations have shown that all these substitutions combined may have a stabilizing effect on the linker domain, which has been demonstrated to influence the enzyme processivity directly and viral replication in Dengue 4 virus *in vitro* models (28, 29). These findings shall be addressed in future studies considering the unrevealed diversity of the YFV in the cell culture and animal models.

A hot spot region of episodic or pervasive positive selection was identified in between codons 2100-2850 of CDS region in YFV genomes of South American genotype I, that was not detected in the West Africa genotype. Interestingly, most of these positively selected sites localize in the NS4B, and NS5 coding regions have also been described in Zika virus from the current epidemics(30). Several studies have demonstrated the role of non-structural proteins in the host innate immune response against flavivirus infection (22, 31-33). Onward, these proteins widely interact with other viral proteins and host molecules (27, 33-35). It is also interesting to note that the 2803

296 position, part of the molecular signature of 2017 YFV, is one of the positively selected
297 sites. Also, two other positions positively selected (826 and 2176), presented variability
298 in the 2017 YFV. These observations support some singularities in the evolutionary
299 dynamics of YFV South American genotype I and also indicate that fixation of some
300 amino acid substitutions in Brazilian 2017 YFV strains might have been driven by
301 positive selection.

302 Since the beginning of the XXI, a striking spreading of the YFV has been
303 occurring in Brazil. The outbreaks formerly constrained to the endemic Amazon and
304 Central-Western regions have reached the South and Southeast of Brazil, where
305 vaccination coverage against YF was insignificant until the explosion of the ongoing
306 outbreak. It has been recently proposed that a YFV strain from Trinidad-Tobago
307 introduced in Brazil and Venezuela in the late 1980s originate all modern-lineages strains
308 belonging to sub-lineages 1D and 1E (12). The main source of variability related to the
309 ancestral lineages is the occurrence of several amino acid substitutions particularly within
310 non-structural viral proteins (12), as observed in the 2017 Brazilian outbreak YFV. All
311 Brazilian 2017 YFV belonged to the sub-lineage 1E and clustered with the Venezuelan
312 strains isolated in the late 2000s, consistent with the notion that ancestral YFV strain
313 responsible for the ongoing Brazilian outbreak would have originated in Venezuela (12).

314 Although Brazilian 2017 YFV strains are most closely related with Venezuelan
315 2004-2010 YFV strains, they share a relatively distant common ancestor traced to 1993
316 (95% HPD: 1987-1997) (Fig. 6). This indicates that the virus may have circulated in
317 endemic South American regions for a long period before being introduced in Southeast
318 Brazil, but the precise pathway of viral dissemination is difficult to elucidate because the
319 paucity of Brazilian YFV sequences sampled from endemic regions over the last 10-15
320 years. We estimate the median T_{MRCA} for the Brazilian 2017 YFV strains at early 2016,

suggesting that the virus circulated for several months in the Southeastern region before the ongoing outbreak was first recognized at December 2016. This pre-detection period of cryptic transmission of YFV in Southeastern Brazil is comparable to that recently estimated for Zika virus in the Northeastern Brazilian region (36).

Bayesian analysis also showed that Brazilian 2017 YFV strains segregate into two sub-clusters, one of them (sub-clade A) containing sequences from both RJ and ES, and the other (sub-clade B) comprising only sequences from RJ whose T_{MRCA} was traced to October 2016. It is also interesting to note that all YFV sequences of RJ that branched within sub-clade A were sampled from sites situated in the Paraíba do Sul basin whose tributaries born on the northern side of the Serra do Mar, a 1,500km long system of mountain ranges and escarpments that runs parallel to the Atlantic Ocean coast in Southeastern Brazil (Fig. 1). By contrast, YFV sequences of RJ that branched within sub-clade B were obtained from locations situated along the Macaé conjugated river basin whose tributaries born on the escarpments of the coastal side of the Serra do Mar.The only exception is the sample H190, which despite originating in the Paraíba do Sul river basin, it clustered in the sub-clade B. Intriguingly, the sampling location of H190 (São Fidelis) is located in the largest discontinuity of the long mountain ranges of the Serra do Mar and this YFV strain branched basally to all other sub-clade B strains. Together, these results support the occurrence of multiple independent introductions of YFV in RJ (probably from both ES and MG) and further indicate at least two main routes of viral dissemination within the state running at the northern and coastal sides of the Serra do Mar. These analyses also point that YFV dissemination through the coastal route in Rio de Janeiro probably started in São Fidelis around late 2016, but more YFV sequences from other Southeastern states are necessary to confirm this conclusion.

Future analysis based on reverse genetic approaches can contribute to establishing the role of amino acid substitutions present in Brazilian 2017 YFV in the viral fitness and transmissibility. It will also be crucial to improving the number of YFV genomes from Brazilian endemic and non-endemic regions in the last years to better understand the epidemiology during recent years.

MATERIAL AND METHODS

Ethics Statements.

This study was reviewed and approved by the Ethics Committee for human research at the Instituto Oswaldo Cruz (IOC) (CAAE 69206217.8.0000.5248), which exempted the need of a specific written informed consent from patients or their legal representatives. The protocols for mosquito rearing as well as handling and blood sampling of NHP were approved by the Institutional Ethics Committee of Animal use at IOC (CEUA licenses LW-34/2014 and L037/2016, respectively). Capture of wild NHPs and mosquitoes were approved by the Brazilian environmental authorities: SISBIO-MMA licenses 54707-137362-2 and 52472-1, and INEA license 012/2016012/2016. No specific permits are needed for conducting mosquito collection in the urban and suburban areas in Southeastern Brazil. This study does not include endangered or protected species.

Mosquito samples

Adult mosquitoes were collected with BG-sentinel adult traps baited with dry ice as a source of CO_2 as well as with an insect net when approaching to humans in the forest, at the forest fringe, and in the modified environment. The insects were immediately frozen in dry ice or N2, transported to the laboratory, identified to species according to Consoli and Lourenço-de-Oliveira (36), and pooled according to species, the number of captured mosquitoes and collecting site and day. Entire bodies of pooled mosquitoes were ground

and treated in Leibovitz L15 medium (Invitrogen) supplemented with 4% Fetal Bovine Serum (FBS), and submitted to the RNA extraction as described elsewhere(37).

Non-human primate samples

Blood samples were taken from the femoral vein of dying NHPs or the cardiac cavity of recently dead NHPs. Samples from howler monkeys were centrifuged (2,000 *g* for 10 min) for obtaining plasma or serum samples stored at low temperature (N_2 or – 80 °C) until RNA extraction. Due to the small amount of blood in the cardiac cavity of dead marmosets, RNA extraction was performed from total blood frozen in dry ice immediately after collection in the field.

Human samples

Blood samples were obtained from patients for diagnosis procedures made at their respective municipal public health ambulatories. Serum samples of suspicious clinical YF cases were sent to the State Central Laboratory in Rio de Janeiro (LACEN-RJ) for molecular and serological analyses. Aliquots of serum samples of YFV laboratory-confirmed cases and negative for Zika virus, Chikungunya virus and Dengue virus infection were selected by the LACEN-RJ staff and stored at - 80 °C until RNA extraction.

YFV RNA extraction, screening for YFV infection by RT-PCR and Nucleotide Sequencing

YFV RNA from mosquito homogenates, blood, and serum samples were obtained by using the QIAamp Viral RNA kit (Qiagen). The RNA samples were eluted in 60 µL of AVE buffer and stored at - 80 °C until use. The YFV RNA was reverse transcribed using the Superscript IV First-Strand Synthesis System (Invitrogen) with random hexamers or specifics primers at 25 °C for 10 min, 55 °C for 10 min and 80 °C for 10 min. Detection of YFV genome was performed by conventional PCR as described

elsewhere (15). Complete YFV genome amplification was carried out by conventional PCR using KAPA HiFi PCR kit (KAPABIOSYSTEMS) under the following conditions: 95 ºC for 3 min, followed by 35 cycles at 98ºC for 20 sec, 65ºC for 15 sec and 72ºC for 45 sec, and a final extension at 72 °C for 1 min 30 sec. The set of primers utilized in PCR and sequencing procedures are listed in the Supplementary files 2 and 3, respectively. Complete genome sequences were deposited in the GenBank database (Table 1). Amplified products were sequenced as previously described (15). The sequenced amplicons were analyzed, and contigs were assembled by using SeqMan Pro v8.1.5 (3), 414 (DNASTAR, Madison, WI). The sequences were manually edited and compared with other sequences available in GenBank (https://www.ncbi.nlm.nih.gov/genbank/). The Molecular Evolutionary Genetics Analysis (MEGA) 7.0 program was used to calculate nucleotide and amino acid distances, as well as to explore the amino acid signatures observed in the YFV strains from the ongoing outbreak in Southeast Brazil.

Comparative modeling, optimization and MD simulation of NS3 pro and NS5 proteins

We performed the modeling of the NS2B-NS3 protein complex and NS5 protein of the 2017 outbreak YFV prototype (Genbank, KY885001) and the 2010 Venezuelan 10A strain (Genbank, KM388816). Initially, we used BLASTP program (https://blast.ncbi.nlm.nih.gov/Blast.cgi?PAGE=Proteins), defining the Protein Data Bank (PDB) as a search set, to select the template structures for comparative modeling. Three PDB structures were used as templates for the NS2B-NS3 protein complex. Template 2VBC (51% identity and 96% of coverage) corresponds to the crystal structure of the NS3 protease-helicase from dengue virus(38). Template 1YKS (96% identity and 70% of coverage) comprises the NS3 helicase domain of the YFV(39). Template 5GJ4 comprises the NS3 protease domain (56% identity and 27 % of coverage) and NS2B

peptide cofactor (42% identity and 31 % of coverage) of Zika virus(40). For the NS5 model generation, a single PDB structure from Japanese Encephalitis virus (4K6M) (19) was used as a template, which shares 60% identity with the YFV sequence. Template and target sequences were then aligned using the PSI-Coffee mode of T-Coffee program(41). One hundred homology models were generated using the standard "auto model" routine of Modeller version 9.18 (42) for each target sequence. Each model was optimized using the variable target function method (VTFM) optimization until accomplishing 300 iterations. Molecular dynamics (MD) optimization, in the slow level mode, was carried out. The full cycle was repeated two times to produce an optimized conformation of the model. The resulting modeled structures were selected according to their discrete optimized protein energy (DOPE) score. The GROMACS version 5.1.2 package(43), was used to carry out minimization using the AMBER99SB ILDN force field(44). A short minimization procedure of 150 steps (100 steps of steepest descent + 50 steps of conjugate-gradient) was performed. Initial and optimized models were evaluated by DOPE, Ramachandran plot and QMean server (Supplementary File 4) (45). The electrostatic potential analysis was conducted using the APBS program(46). Atomic partial charges and atomic radii parameters from the Amber force field were assigned using the PDB2PQR server (47). Figures of sequence alignments were rendered using ALINE (48), and 3D structures were generated using UCSF Chimera and PyMol.

Molecular dynamics simulations were carried out using the GROMACS package, with the AMBER99SB-ILDN force field. Protonation states were assigned using pdb2pqr software, and the zinc-coordinating cysteine residues were manually deprotonated. The models were further optimized prior to the MD runs, through 5.0×10^6 steps of the Steepest Descent (with and without heavy atom restraints) and Conjugate Gradients algorithms. The systems were then run, under an NPT ensemble, for 500 ps with restraints

445 and 2.0 x 10^5 ps without restraints. The V-rescale thermostat and Berendsen barostat
446 were used for temperature and pressure control, respectively. The 2010 and 2017 strains
447 and replicas were simulated at 297 and 310 K for a total of 8 runs and 1.6 x 10^6 ps.
448 Analysis was made over the final 150 ns of the production runs.

449 **PrM/E phylogenetic analysis**

450 A 666-nucleotide sequence consisting of the last 108 nucleotides of the prM gene,
451 the entire M gene (225 nucleotides), and the first 333 nucleotides of the E gene was used
452 to established genotype the YFV strains, as previously described(5). In addition to the
453 sequences obtained in the current study, a set of sequences of the prM/E junction fragment
454 were selected using the Blast tool (https://blast.ncbi.nlm.nih.gov/Blast.cgi) and all
455 sequences were aligned using Molecular Evolutionary Genetics Analysis (MEGA)
456 7.0(49). The phylogenetic tree was generated by the Neighbor-joining method (50) using
457 a matrix of genetic distances established under the Kimura-two parameter model (51).
458 The robustness of each node was assessed by bootstrap resampling (2,000 replicates) (52).
459 The homologous region (prM/E) of a dengue virus strain available at the GenBank
460 database (AF349753) was used as an outgroup.

461 **Selection pressure analyses**

462 Two datasets of sequences were determined: a) Dataset South America I (Set SAI)
463 with all complete CDS of South American YFV stains available in the GenBank plus
464 sequences obtained in the current study (N=32); b) Dataset West Africa (Set WA), with
465 complete CDS from West Africa genotype YFV strains available in the Genbank. The
466 reason to generate these two datasets was that West African genotype has a closest genetic
467 relationship with South America genotype I (5), and only two CDS from YFV strains
468 belonging to South America genotype II are available in the GenBank to date. Datasets
469 were aligned using Bioedit v7.2.3 (53) and were tested for positive selection by using the

online adaptive evolution server DATAMONKEY(54, 55). The ratio of non-synonymous to synonymous substitutions (dN/dS) per codon sites were estimated using four different methods, SLAC - Single Likelihood Ancestor Counting, FEL - Fixed Effects Likelihood(56), MEME - Mixed Effects Model of Evolution(57) and FUBAR - Fast Unbiased Bayesian Approximate(58). The analysis was run based on neighbor-joining tree and significant P-value (< 0.1). The automated model selection tool available in the server was used for selection of appropriate nucleotide substitution bias model for both datasets.

Evolutionary analyses

Complete coding regions sequences (CDS - 10,239 nt in length) of YFV of American origin (South America genotypes I and II), with a known date of isolation, were obtained from the GenBank database (www.ncbi.nlm.nih.gov). Retrieved sequences were aligned together with sequences obtained in the current study using MEGA 7.0 (49). The nucleotide substitution rate and time of the most recent common ancestor (T_{MRCA}) of American YFV strains were estimated using the Markov chain Monte Carlo (MCMC) algorithm implemented in the BEAST v1.8.3 package(59, 60) with BEAGLE (61) to improve run-time. The best-fit nucleotide substitution model, a relaxed uncorrelated lognormal molecular clock model(62), and a Bayesian Skyline coalescent tree prior(63) were used. The uncertainty of parameter estimates was assessed after excluding the initial 10% of the run by calculating the Effective Sample Size (ESS) and the 95% Highest Probability Density (HPD) values, respectively, using TRACER v1.6 program(64). TreeAnnotator v1.7.5 (60) and FigTree v1.4.0 (65) were used to summarize the posterior tree distribution and to visualize the annotated Maximum Clade Credibility (MCC) tree, respectively.

Acknowledgments

To Monique Albuquerque Motta for the help on mosquito identification; Iule de Souza Bonelli, Marcelo Quinteka Gomes, Lidiane S. R. Menezes, Nathália D. Furtado, Stephanie O. D. da Cruz and Adalgiza as Silva Rocha for technical assistance; Heloisa Diniz and Leônidas Leite Santos for the help with illustrations; Alexandre Otávio Chieppe, Ana Paula Martins Brandão, Carlos Augusto Ferandes (Secretaria Estadual de Saúde do Rio de Janeiro) Alessandro Pecego M. Romano (Grupo Técnico de Vigilância de Arboviroses) and Roberta Gomes de Carvalho (Programa Nacional de Controle da Dengue) Brazilian Ministry of Health, Gilsa Aparecida P. Rodrigues (Secretaria de Saúde do Estado do Espírito Santo), Gilton Luiz Almada (Centro de Informação Estratégica de Vigilância em Saúde-ES) for the access to epidemiological data and support for the field work; Marilza L. Lange (Secretaria Municipal de Saúde, Municipality of Domingos Martins), Luciano L. Salles (Vigilância em Saúde, Municipality of Ibatiba) Agenor Barbosa de Oliveira, Marcelo dos Santos Rosário, Mauro Cesar Louzada, Max Mauro dos Santos Coelho for their assistance in field collections in Espírito Santo. Alexandre Bezerra de Souza and Vicente Klonowski (Atalaia Park), Romenique de Lemos Araújo, Luiz Ribeiro Nogueira and Raquel Giri Faria (Environmental Guard) and Macaé prefecture for their support in collecting samples. Raul Henrique Rafael and Ana Luiza Quijada for access to the Guapimirim sample; Cassia Schitino de Carvalho Gomes and Paulo Vitor Araújo Gomes for access to the Carmo samples.

Competing interests

The authors declare that no competing interests exist.

517 REFERENCES

518 1. Barnett, E. D., Yellow fever: epidemiology and prevention. *Clin Infect Dis* **44**,
519 850-856 (2007), 10.1086/511869

520 2. Monath, T. P., Vasconcelos, P. F., Yellow fever. *J Clin Virol* **64**, 160-173 (2015),
521 10.1016/j.jcv.2014.08.030

522 3. Weaver, S. C., Reisen, W. K., Present and future arboviral threats. *Antiviral Res*
523 **85**, 328-345 (2010), 10.1016/j.antiviral.2009.10.008

524 4. Vasconcelos, P. F., Monath, T. P., Yellow Fever Remains a Potential Threat to
525 Public Health. *Vector Borne Zoonotic Dis* **16**, 566-567 (2016),
526 10.1089/vbz.2016.2031

527 5. Bryant, J. E., Holmes, E. C., Barrett, A. D., Out of Africa: a molecular perspective
528 on the introduction of yellow fever virus into the Americas. *PLoS Pathog* **3**, e75
529 (2007), 10.1371/journal.ppat.0030075

530 6. Mutebi, J. P., Wang, H., Li, L., Bryant, J. E., Barrett, A. D., Phylogenetic and
531 evolutionary relationships among yellow fever virus isolates in Africa. *J Virol* **75**,
532 6999-7008 (2001), 10.1128/JVI.75.15.6999-7008.2001

533 7. Staples, J. E., Monath, T. P., Yellow fever: 100 years of discovery. *JAMA* **300**,
534 960-962 (2008), 10.1001/jama.300.8.960

535 8. Nunes, M. R., Palacios, G., Cardoso, J. F., Martins, L. C., Sousa, E. C., Jr., de
536 Lima, C. P., Medeiros, D. B., Savji, N., Desai, A., Rodrigues, S. G., Carvalho, V.
537 L., Lipkin, W. I., Vasconcelos, P. F., Genomic and phylogenetic characterization
538 of Brazilian yellow fever virus strains. *J Virol* **86**, 13263-13271 (2012),
539 10.1128/JVI.00565-12

9. Vasconcelos, P. F., Bryant, J. E., da Rosa, T. P., Tesh, R. B., Rodrigues, S. G., Barrett, A. D., Genetic divergence and dispersal of yellow fever virus, Brazil. *Emerg Infect Dis* **10**, 1578-1584 (2004), 10.3201/eid1009.040197

10. Romano, A. P., Costa, Z. G., Ramos, D. G., Andrade, M. A., Jayme Vde, S., Almeida, M. A., Vettorello, K. C., Mascheretti, M., Flannery, B., Yellow Fever outbreaks in unvaccinated populations, Brazil, 2008-2009. *PLoS Negl Trop Dis* **8**, e2740 (2014), 10.1371/journal.pntd.0002740

11. de Souza, R. P., Foster, P. G., Sallum, M. A., Coimbra, T. L., Maeda, A. Y., Silveira, V. R., Moreno, E. S., da Silva, F. G., Rocco, I. M., Ferreira, I. B., Suzuki, A., Oshiro, F. M., Petrella, S. M., Pereira, L. E., Katz, G., Tengan, C. H., Siciliano, M. M., Dos Santos, C. L., Detection of a new yellow fever virus lineage within the South American genotype I in Brazil. *J Med Virol* **82**, 175-185 (2010), 10.1002/jmv.21606

12. Mir, D., Delatorre, E., Bonaldo, M., Lourenço-de-Oliveira, R., Vicente, A. C., Bello, G., Phylodynamics of Yellow Fever Virus in the Americas: new insights into the origin of the 2017 Brazilian outbreak. *Scientific Reports* **7**, (2017), 10.1038/s41598-017-07873-7

13. Health, B. M. o., COES -Febre amarela. Informe 42/2-17, (2017), http://portalarquivos.saude.gov.br/images/pdf/2017/maio/26/COES-FEBRE-AMARELA-INFORME-42.pdf

14. Organization, P. A. H., Epidemiological Update -Yellow Fever, (2017), http://www.paho.org/hq/index.php?option=com_docman&task=doc_view&Itemid=270&gid=40841&lang=en

15. Bonaldo, M. C., Gomez, M. M., Dos Santos, A. A., Abreu, F. V. S., Ferreira-de-Brito, A., Miranda, R. M., Castro, M. G., Lourenco-de-Oliveira, R., Genome

analysis of yellow fever virus of the ongoing outbreak in Brazil reveals polymorphisms. *Mem Inst Oswaldo Cruz* **112**, 447-451 (2017), 10.1590/0074-02760170134

16. Luo, D., Vasudevan, S. G., Lescar, J., The flavivirus NS2B-NS3 protease-helicase as a target for antiviral drug development. *Antiviral Res* **118**, 148-158 (2015), 10.1016/j.antiviral.2015.03.014

17. Khromykh, A. A., Sedlak, P. L., Westaway, E. G., trans-Complementation analysis of the flavivirus Kunjin ns5 gene reveals an essential role for translation of its N-terminal half in RNA replication. *J Virol* **73**, 9247-9255 (1999), https://www.ncbi.nlm.nih.gov/pubmed/10516033)

18. Koonin, E. V., Computer-assisted identification of a putative methyltransferase domain in NS5 protein of flaviviruses and lambda 2 protein of reovirus. *J Gen Virol* **74 (Pt 4)**, 733-740 (1993), 10.1099/0022-1317-74-4-733

19. Lu, G., Gong, P., Crystal Structure of the full-length Japanese encephalitis virus NS5 reveals a conserved methyltransferase-polymerase interface. *PLoS Pathog* **9**, e1003549 (2013), 10.1371/journal.ppat.1003549

20. El Sahili, A., Lescar, J., Dengue Virus Non-Structural Protein 5. *Viruses* **9**, (2017), 10.3390/v9040091

21. Laurent-Rolle, M., Morrison, J., Rajsbaum, R., Macleod, J. M. L., Pisanelli, G., Pham, A., Ayllon, J., Miorin, L., Martinez, C., tenOever, B. R., Garcia-Sastre, A., The interferon signaling antagonist function of yellow fever virus NS5 protein is activated by type I interferon. *Cell Host Microbe* **16**, 314-327 (2014), 10.1016/j.chom.2014.07.015

588 22. Cumberworth, S. L., Clark, J. J., Kohl, A., Donald, C. L., Inhibition of type I
589 interferon induction and signalling by mosquito-borne flaviviruses. *Cell*
590 *Microbiol* **19**, (2017), 10.1111/cmi.12737
591 23. Dorigatti, I., Hamlet, A., Aguas, R., Cattarino, L., Cori, A., Donnelly, C. A.,
592 Garske, T., Imai, N., Ferguson, N. M., International risk of yellow fever spread
593 from the ongoing outbreak in Brazil, December 2016 to May 2017. *Euro Surveill*
594 **22**, (2017), 10.2807/1560-7917.ES.2017.22.28.30572
595 24. Couto-Lima, D., Madec, Y., Bersot, M. I., Campos, S. S., Motta, M. A., Santos,
596 F. B. D., Vazeille, M., Vasconcelos, P., Lourenco-de-Oliveira, R., Failloux, A. B.,
597 Potential risk of re-emergence of urban transmission of Yellow Fever virus in
598 Brazil facilitated by competent Aedes populations. *Sci Rep* **7**, 4848 (2017),
599 10.1038/s41598-017-05186-3
600 25. Carpp, L. N., Galler, R., Bonaldo, M. C., Interaction between the yellow fever
601 virus nonstructural protein NS3 and the host protein Alix contributes to the release
602 of infectious particles. *Microbes Infect* **13**, 85-95 (2011),
603 10.1016/j.micinf.2010.10.010
604 26. Patkar, C. G., Kuhn, R. J., Yellow Fever virus NS3 plays an essential role in virus
605 assembly independent of its known enzymatic functions. *J Virol* **82**, 3342-3352
606 (2008), 10.1128/JVI.02447-07
607 27. Teramoto, T., Balasubramanian, A., Choi, K. H., Padmanabhan, R., Serotype-
608 specific interactions among functional domains of dengue virus 2 nonstructural
609 proteins (NS) 5 and NS3 are crucial for viral RNA replication. *J Biol Chem* **292**,
610 9465-9479 (2017), 10.1074/jbc.M117.775643
611 28. Lim, S. P., Koh, J. H., Seh, C. C., Liew, C. W., Davidson, A. D., Chua, L. S.,
612 Chandrasekaran, R., Cornvik, T. C., Shi, P. Y., Lescar, J., A crystal structure of

the dengue virus non-structural protein 5 (NS5) polymerase delineates interdomain amino acid residues that enhance its thermostability and de novo initiation activities. *J Biol Chem* **288**, 31105-31114 (2013), 10.1074/jbc.M113.508606

29. Zhao, Y., Soh, T. S., Zheng, J., Chan, K. W., Phoo, W. W., Lee, C. C., Tay, M. Y., Swaminathan, K., Cornvik, T. C., Lim, S. P., Shi, P. Y., Lescar, J., Vasudevan, S. G., Luo, D., A crystal structure of the Dengue virus NS5 protein reveals a novel inter-domain interface essential for protein flexibility and virus replication. *PLoS Pathog* **11**, e1004682 (2015), 10.1371/journal.ppat.1004682

30. Sironi, M., Forni, D., Clerici, M., Cagliani, R., Nonstructural Proteins Are Preferential Positive Selection Targets in Zika Virus and Related Flaviviruses. *PLoS Negl Trop Dis* **10**, e0004978 (2016), 10.1371/journal.pntd.0004978

31. Mathew, A., Townsley, E., Ennis, F. A., Elucidating the role of T cells in protection against and pathogenesis of dengue virus infections. *Future Microbiol* **9**, 411-425 (2014), 10.2217/fmb.13.171

32. Schlesinger, J. J., Foltzer, M., Chapman, S., The Fc portion of antibody to yellow fever virus NS1 is a determinant of protection against YF encephalitis in mice. *Virology* **192**, 132-141 (1993), 10.1006/viro.1993.1015

33. Wu, R. H., Tsai, M. H., Tsai, K. N., Tian, J. N., Wu, J. S., Wu, S. Y., Chern, J. H., Chen, C. H., Yueh, A., Mutagenesis of Dengue Virus Protein NS2A Revealed a Novel Domain Responsible for Virus-Induced Cytopathic Effect and Interactions between NS2A and NS2B Transmembrane Segments. *J Virol* **91**, (2017), 10.1128/JVI.01836-16

34. Le Breton, M., Meyniel-Schicklin, L., Deloire, A., Coutard, B., Canard, B., de Lamballerie, X., Andre, P., Rabourdin-Combe, C., Lotteau, V., Davoust, N.,

638 Flavivirus NS3 and NS5 proteins interaction network: a high-throughput yeast
639 two-hybrid screen. *BMC Microbiol* **11**, 234 (2011), 10.1186/1471-2180-11-234
640 35. Zou, J., Lee le, T., Wang, Q. Y., Xie, X., Lu, S., Yau, Y. H., Yuan, Z., Geifman
641 Shochat, S., Kang, C., Lescar, J., Shi, P. Y., Mapping the Interactions between the
642 NS4B and NS3 proteins of dengue virus. *J Virol* **89**, 3471-3483 (2015),
643 10.1128/JVI.03454-14
644 36. Faria, N. R., Azevedo, R., Kraemer, M. U. G., Souza, R., Cunha, M. S., Hill, S.
645 C., Theze, J., Bonsall, M. B., Bowden, T. A., Rissanen, I., Rocco, I. M., Nogueira,
646 J. S., Maeda, A. Y., Vasami, F., Macedo, F. L. L., Suzuki, A., Rodrigues, S. G.,
647 Cruz, A. C. R., Nunes, B. T., Medeiros, D. B. A., Rodrigues, D. S. G., Queiroz,
648 A. L. N., da Silva, E. V. P., Henriques, D. F., da Rosa, E. S. T., de Oliveira, C. S.,
649 Martins, L. C., Vasconcelos, H. B., Casseb, L. M. N., Simith, D. B., Messina, J.
650 P., Abade, L., Lourenco, J., Alcantara, L. C. J., de Lima, M. M., Giovanetti, M.,
651 Hay, S. I., de Oliveira, R. S., Lemos, P. D. S., de Oliveira, L. F., de Lima, C. P.
652 S., da Silva, S. P., de Vasconcelos, J. M., Franco, L., Cardoso, J. F., Vianez-Junior,
653 J., Mir, D., Bello, G., Delatorre, E., Khan, K., Creatore, M., Coelho, G. E., de
654 Oliveira, W. K., Tesh, R., Pybus, O. G., Nunes, M. R. T., Vasconcelos, P. F. C.,
655 Zika virus in the Americas: Early epidemiological and genetic findings. *Science*
656 **352**, 345-349 (2016), 10.1126/science.aaf5036
657 37. Consoli, R. A. G. B., Oliveira, R. L., *Principais mosquitos de importância*
658 *sanitária no Brasil*. (Editora FIOCRUZ, Rio de Janeiro, 1994), pp. 228.
659 38. Ferreira-de-Brito, A., Ribeiro, I. P., Miranda, R. M., Fernandes, R. S., Campos, S.
660 S., Silva, K. A., Castro, M. G., Bonaldo, M. C., Brasil, P., Lourenco-de-Oliveira,
661 R., First detection of natural infection of Aedes aegypti with Zika virus in Brazil

and throughout South America. *Mem Inst Oswaldo Cruz* **111**, 655-658 (2016), 10.1590/0074-02760160332

39. Luo, D., Xu, T., Hunke, C., Gruber, G., Vasudevan, S. G., Lescar, J., Crystal structure of the NS3 protease-helicase from dengue virus. *J Virol* **82**, 173-183 (2008), 10.1128/JVI.01788-07

40. Wu, J., Bera, A. K., Kuhn, R. J., Smith, J. L., Structure of the Flavivirus helicase: implications for catalytic activity, protein interactions, and proteolytic processing. *J Virol* **79**, 10268-10277 (2005), 10.1128/JVI.79.16.10268-10277.2005

41. Phoo, W. W., Li, Y., Zhang, Z., Lee, M. Y., Loh, Y. R., Tan, Y. B., Ng, E. Y., Lescar, J., Kang, C., Luo, D., Structure of the NS2B-NS3 protease from Zika virus after self-cleavage. *Nat Commun* **7**, 13410 (2016), 10.1038/ncomms13410

42. Di Tommaso, P., Moretti, S., Xenarios, I., Orobitg, M., Montanyola, A., Chang, J. M., Taly, J. F., Notredame, C., T-Coffee: a web server for the multiple sequence alignment of protein and RNA sequences using structural information and homology extension. *Nucleic Acids Res* **39**, W13-17 (2011), 10.1093/nar/gkr245

43. Webb, B., Sali, A., in *Protein Structure Prediction,* D. Kihara, Ed. (Springer New York, New York, 2014), vol. 1137, pp. 1-15.

44. Abraham, M. K., Murtola, T., Schulz, R., Páll, S., Smith, J. C., Hess, H., Lindahl, E., GROMACS: High performance molecular simulations through multi-level parallelism from laptops to supercomputers. *SoftwareX* **1-2**, 19-25 (2015), 10.1016/j.softx.2015.06.001

45. Lindorff-Larsen, K., Piana, S., Palmo, K., Maragakis, P., Klepeis, J. L., Dror, R. O., Shaw, D. E., Improved side-chain torsion potentials for the Amber ff99SB protein force field. *Proteins* **78**, 1950-1958 (2010), 10.1002/prot.22711

686 46. Benkert, P., Kunzli, M., Schwede, T., QMEAN server for protein model quality
687 estimation. *Nucleic Acids Res* **37**, W510-514 (2009), 10.1093/nar/gkp322
688 47. Baker, N. A., Sept, D., Joseph, S., Holst, M. J., McCammon, J. A., Electrostatics
689 of nanosystems: application to microtubules and the ribosome. *Proc Natl Acad*
690 *Sci U S A* **98**, 10037-10041 (2001), 10.1073/pnas.181342398
691 48. Dolinsky, T. J., Nielsen, J. E., McCammon, J. A., Baker, N. A., PDB2PQR: an
692 automated pipeline for the setup of Poisson-Boltzmann electrostatics calculations.
693 *Nucleic Acids Res* **32**, W665-667 (2004), 10.1093/nar/gkh381
694 49. Bond, C. S., Schuttelkopf, A. W., ALINE: a WYSIWYG protein-sequence
695 alignment editor for publication-quality alignments. *Acta Crystallogr D Biol*
696 *Crystallogr* **65**, 510-512 (2009), 10.1107/S0907444909007835
697 50. Kumar, S., Stecher, G., Tamura, K., MEGA7: Molecular Evolutionary Genetics
698 Analysis Version 7.0 for Bigger Datasets. *Mol Biol Evol* **33**, 1870-1874 (2016),
699 10.1093/molbev/msw054
700 51. Saitou, N., Nei, M., The neighbor-joining method: a new method for
701 reconstructing phylogenetic trees. *Mol Biol Evol* **4**, 406-425 (1987),
702 https://www.ncbi.nlm.nih.gov/pubmed/3447015)
703 52. Kimura, M., A simple method for estimating evolutionary rates of base
704 substitutions through comparative studies of nucleotide sequences. *J Mol Evol* **16**,
705 111-120 (1980), https://www.ncbi.nlm.nih.gov/pubmed/7463489)
706 53. Felsenstein, J., Confidence Limits on Phylogenies: An Approach Using the
707 Bootstrap. *Evolution* **39**, 783-791 (1985), 10.1111/j.1558-5646.1985.tb00420.x
708 54. Hall, T. A., A User-Friendly Biological Sequence Alignment Editor and Analysis
709 Program for Windows 95/98/NT. *Nucleic Acids Symposium Series* **41**, 95-98
710 (1999),

711 55. Delport, W., Poon, A. F., Frost, S. D., Kosakovsky Pond, S. L., Datamonkey 2010:
712 a suite of phylogenetic analysis tools for evolutionary biology. *Bioinformatics* **26**,
713 2455-2457 (2010), 10.1093/bioinformatics/btq429
714 56. Pond, S. L., Frost, S. D., Datamonkey: rapid detection of selective pressure on
715 individual sites of codon alignments. *Bioinformatics* **21**, 2531-2533 (2005),
716 10.1093/bioinformatics/bti320
717 57. Kosakovsky Pond, S. L., Frost, S. D., Not so different after all: a comparison of
718 methods for detecting amino acid sites under selection. *Mol Biol Evol* **22**, 1208-
719 1222 (2005), 10.1093/molbev/msi105
720 58. Murrell, B., Wertheim, J. O., Moola, S., Weighill, T., Scheffler, K., Kosakovsky
721 Pond, S. L., Detecting individual sites subject to episodic diversifying selection.
722 *PLoS Genet* **8**, e1002764 (2012), 10.1371/journal.pgen.1002764
723 59. Murrell, B., Moola, S., Mabona, A., Weighill, T., Sheward, D., Kosakovsky Pond,
724 S. L., Scheffler, K., FUBAR: a fast, unconstrained bayesian approximation for
725 inferring selection. *Mol Biol Evol* **30**, 1196-1205 (2013), 10.1093/molbev/mst030
726 60. Drummond, A. J., Rambaut, A., BEAST: Bayesian evolutionary analysis by
727 sampling trees. *BMC Evol Biol* **7**, 214 (2007), 10.1186/1471-2148-7-214
728 61. Drummond, A. J., Suchard, M. A., Xie, D., Rambaut, A., Bayesian phylogenetics
729 with BEAUti and the BEAST 1.7. *Mol Biol Evol* **29**, 1969-1973 (2012),
730 10.1093/molbev/mss075
731 62. Suchard, M. A., Rambaut, A., Many-core algorithms for statistical phylogenetics.
732 *Bioinformatics* **25**, 1370-1376 (2009), 10.1093/bioinformatics/btp244
733 63. Drummond, A. J., Ho, S. Y., Phillips, M. J., Rambaut, A., Relaxed phylogenetics
734 and dating with confidence. *PLoS Biol* **4**, e88 (2006),
735 10.1371/journal.pbio.0040088

64. Drummond, A. J., Rambaut, A., Shapiro, B., Pybus, O. G., Bayesian coalescent inference of past population dynamics from molecular sequences. *Mol Biol Evol* **22**, 1185-1192 (2005), 10.1093/molbev/msi103

65. Rambaut, A., Suchard, M., Drummond, A., Tracer v1.6. , (2013), <http://tree.bio.ed.ac.uk/software/tracer/>

66. Rambaut, A., FigTree v1.4., (2014), <http://tree.bio.ed.ac.uk/software/figtree/>

743 **Figure Legends**

744

745 Figure 1. The spatiotemporal spread of the yellow fever outbreak in Southeast Brazil from
746 December 2016 to May 2017, and geographical origins of the yellow fever virus (YFV)
747 samples according to states, river basins, hosts, and YFV sub-clades A (red) and B
748 (green). The black square corresponds to the H189 sample whose only partial sequences
749 of the YFV genome were obtained. Brazilian states: ES (Espírito Santo), MG (Minas
750 Gerais), RJ (Rio de Janeiro) and SP: (São Paulo). Hatched areas correspond to the Great
751 Metropolitan (GM) areas of Rio de Janeiro and Vitória.

752

753 Figure 2. Amino acid (aa) differences revealed by the alignment of the precursor
754 polyproteins of 32 yellow fever (YF) viruses of the South America genotype I. On the
755 left of the alignment data, the identification of lineage, sub-lineages and yellow fever
756 virus (YFV) sequences are supplied. On the top of the alignment, the YF viral proteins
757 positions are indicated along with the aa positions of amino acid differences. The orange-
758 highlighted aa indicates the position of aa shared only by all YF sequences from the
759 ongoing outbreak in Brazil. Amino acid residues highlighted in blue indicate aa changes
760 present in YF strains from the current outbreak, first described in the current study. The
761 "+" symbol indicates the sites under positive selection in the YF polyprotein.

762

763 Figure 3. Tridimensional models obtained by comparative modeling of the NS2B-NS3
764 protein complex. Cartoon and surface electrostatic potential representation of R121K
765 substitution (A, B**)**, whole complex (C, D), and E88D substitution (E, F)**.** The molecular
766 surface is colored according to electrostatic potential, where red, white and blue

767 correspond to acidic, neutral and basic potentials, respectively. NS2B is shown in green.
768 Thick black lines represent hydrogen bonds (A, B, E, F)
769
770 Figure 4**.** Tridimensional structural models obtained by comparative modeling of NS5
771 protein. (A) Cartoon representation of NS5 protein. Amino acid substitutions and binding
772 site residues are shown in the sticks and colored according to the legend. (B) Cavities of
773 NS5 protein. Amino acid substitution sites are shown in red.
774
775 Figure 5. Codons of the yellow fever virus under positive selection in South America
776 genotype I (top), and West Africa genotype (bottom). The Y-axis represents normalized
777 dN-dS (non-synonymous substitutions minus synonymous substitution), and the X-axis
778 represents codon positions. The region between codon positions 2100 and 2850 is
779 highlighted inside a gray rectangle. Positively selected sites are shown with the color code
780 that appeared at the bottom of the figure.
781
782 Figure 6. Phylogenetic evolutionary analysis based on the yellow fever virus (YFV)
783 complete coding region. (A) Time-scaled Bayesian MCC tree of YFV CDS. The color
784 code is explained at the left of the figure. Names and accession numbers of the strains are
785 shown in Fig. 6 – Fig. Supplement 1. (B) YFV from the ongoing Southeast Brazilian
786 outbreak.
787
788 **Figures –Figure Supplement legends**
789
790 Figure 2- Figure Supplement 1. Phylogenetic analysis based on the prM/E junction region
791 of yellow fever virus (YFV) strains analyzed in the current study and YFV sequences

792 retrieved from the National Centre for Biotechnology Information (NCBI). Only
793 bootstrap values up to 70% are shown. YFV genotypes are shown at the right side of the
794 figure. The scale bar at the bottom represents 0.1 substitutions per nucleotide position
795 (nt.subst/site). YFV from the 2017 ongoing Southeast Brazilian outbreak are marked with
796 a filled triangle (mosquito strains), filled square (human strains) and filled circle (non-
797 human primates strains).
798 Figure 2- Figure Supplement 2. Phylogenetic analysis based on the NS3 (A) and NS5 (B)
799 encoding region of yellow fever virus (YFV) strains analyzed in the current study and 21
800 YFV sequences retrieved from the National Centre for Biotechnology Information
801 (NCBI). Only bootstrap values up to 70% are shown. The scale bar at the bottom
802 represents 0.1 substitutions per nucleotide position (nt.subst/site). YFV from the 2017
803 ongoing Southeast Brazilian outbreak are marked with an empty circle. South America
804 genotype I and sub-clade 1E are shown at the right side.
805
806 Figure3 - Figure Supplement 1. Multiple sequence alignment of the NS3 protein sequence
807 belonging to the 2017 Brazilian yellow fever virus (strain ES505), 2010 Venezuelan 10A
808 strain and the three templates used in comparative modeling experiment. Black and gray
809 filled positions of the alignment represent fully and partially conserved residues,
810 respectively. Red outline highlights the amino acid found in the 2017 Brazilian strain.
811 Green outline highlights the positions of the active site residues.
812
813 Figure 4 - Figure Supplement 1. Multiple sequence alignment of the NS5 protein
814 sequence belonging to the 2017 Brazilian yellow fever virus (strain ES505), 2010
815 Venezuelan 10A strain and the template used in comparative modeling experiment. Black
816 and gray filled positions of the alignment represent fully and partially conserved residues,

817 respectively. Red outline highlights the amino acid found in the 2017 Brazilian strain.
818 Pink, yellow and green outlines highlight the positions of residues found in the active site,
819 GTP binding site, and SAM binding site, respectively.
820
821 Figure 4 - Figure Supplement 2. The surface electrostatic potential of NS5 protein. The
822 molecular surface is colored according to electrostatic potential, where red, white and
823 blue correspond to acidic, neutral and basic potentials, respectively.
824 Figure 4 - Figure Supplement 3. Root mean square fluctuation plots of the final 150 ns of
825 each NS5 MD production run. The systems were run in replicates with distinct random
826 seeds for initial velocities generation. Temperatures of 297 and 310 K were used. The last
827 column (Relative) represents the subtraction of the calculated fluctuations of 2010 from
828 the 2017 values. The vertical dashed line marks the hinge domain. Fluctuations were
829 calculated with GROMACS software and plotted using R.
830
831 Figure 5 - Figure Supplement 1. Positively selected sites in yellow fever virus (YFV)
832 polyprotein from South American genotype I (top) and West African (bottom). Sites,
833 where the non-synonymous substitution occurred in YFV 2017 (top) are shown with a
834 gray shadow. a- Sites supported by one method (FEL or MEME); b- sites supported by
835 two methods (MEME/FUBAR or fel/fubar); c- site supported by three methods
836 FEL/MEME/FUBAR.
837
838 Figure 6 – Figure supplement 1.. Yellow fever virus strains used in the Time-scaled
839 Bayesian MCC tree.
840

Table 1. YFV samples collected in the 2017 Brazilian outbreak

Host	Sample ID - (Genbank accession number)	Date of collection	Local	geographic coordinates
Hg. leucocelaenus	PA193 - (MF423373)	21/02/2017	Areinha, Domingos Martins - ES	20º17'08"S 40º50'15" W
Hg. janthinomys	PA196 - (MF423374)	23/02/2017	Areinha, Domingos Martins - ES	20º17'08"S 40º50'15"W
Alouatta clamitans (howler-monkey)	ES-504* - (KY885000)	20/02/2017	Areinha, Domingos Martins - ES	20º17'08"S 40º50'15"W
	ES-505* - (KY885001)	22/02/2017	Areinha, Domingos Martins - ES	20º17'08"S 40º50'15"W
	RJ87 - (MF423375)	04/04/2017	Atalaia, Macaé - RJ	22°18'31.6"S 42°00'01.7"W
	RJ94 - (MF423376)	13/04/2017	Cabeceira do Sana, Macaé - RJ	22°14'23.1"S 42°09'05.0"W
	RJ95 - (MF423377)	19/04/2017	Santa Fé, Carmo - RJ	21°53'05.0"S 42°32'29.7"W
	RJ96 - (MF423378)	19/04/2017	Santa Fé, Carmo - RJ	21°53'05.0"S 42°32'29.7"W
Callithrix jacchus/penicillata (marmoset)	RJ97- (MF538785)	21/04/2017	Araras, Petrópolis - RJ	22°23'51.1"S 43°10'56.5"W
	RJ104 - (MF538786)	05/06/2017	Caneca Fina, Guapimirim - RJ	22°29'35.9"S 42°56'58.9"W
Human cases	H189 **	18/04/2017	Bananal, Maricá - RJ	22°55'25.3"S 42°43'17.1"W
	H190 - (MF538782)	16/03/2017	São Fidélis - RJ	21°38'17.2"S 41°45'49.2"W
	H191 - (MF538783)	18/03/2017	Casimiro de Abreu - RJ	22°29'10.5"S 42°12'06.2"W
	H196 - (MF538784)	26/02/2017	Porciúncula - RJ	20°49'17.5"S 41°54'38.6"W
	H199 - (MF434851)	25/04/2017	Silva Jardim - RJ	22°27'42.9"S 42°18'28.6"W

*YFV ES504 and ES505 previously described (13); ** partial genome sequence

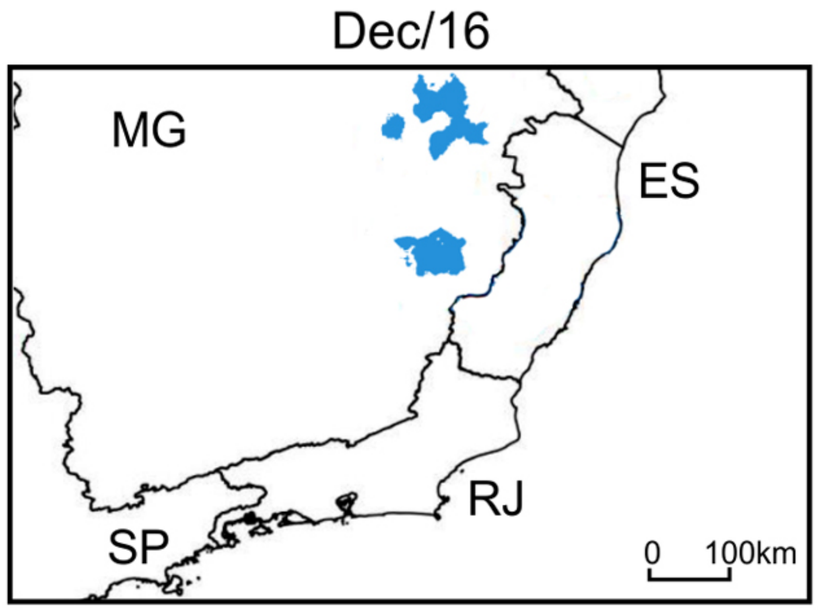

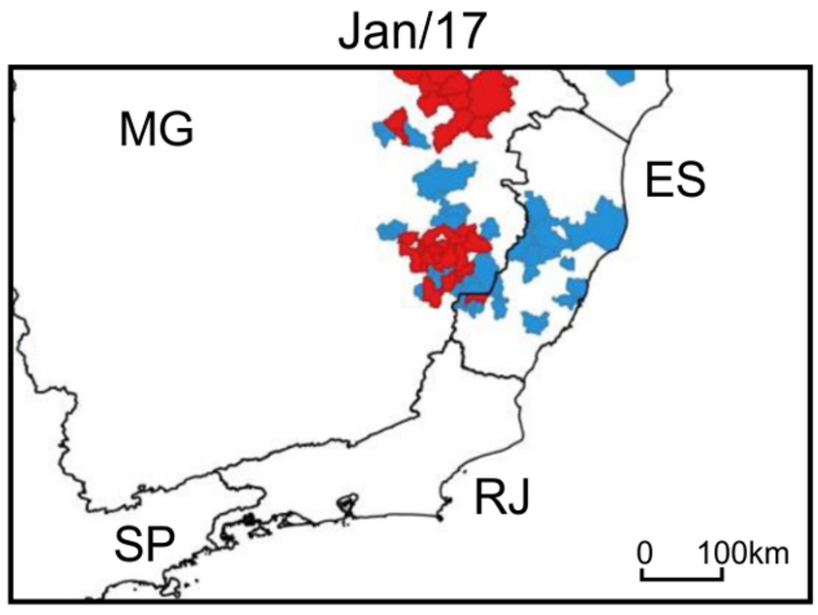

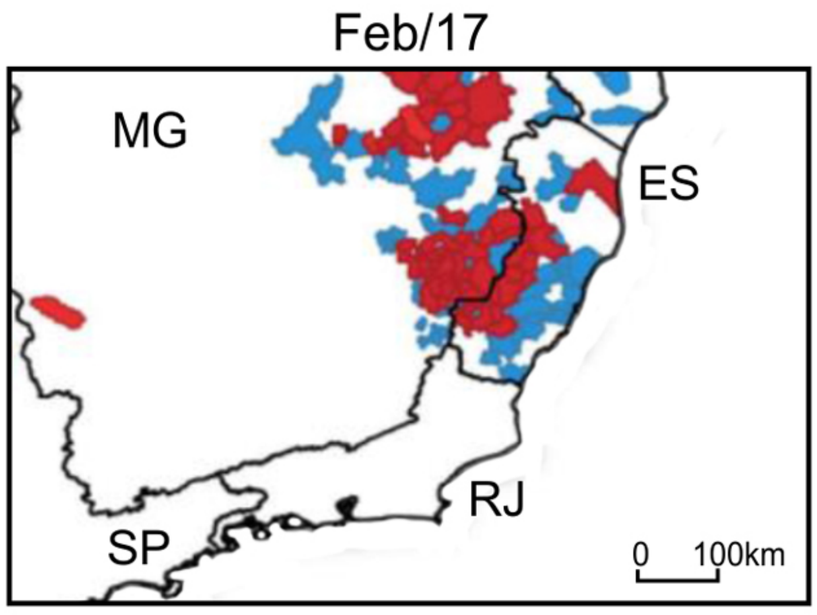

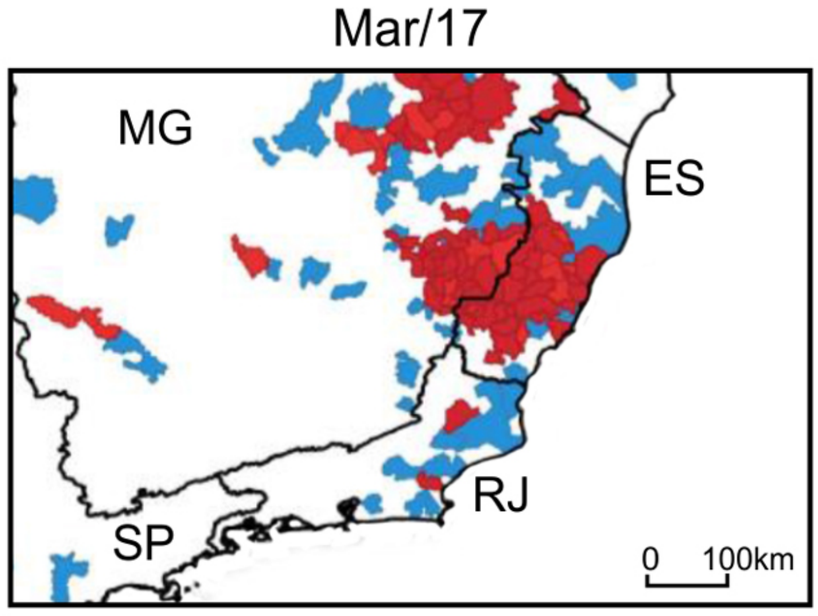

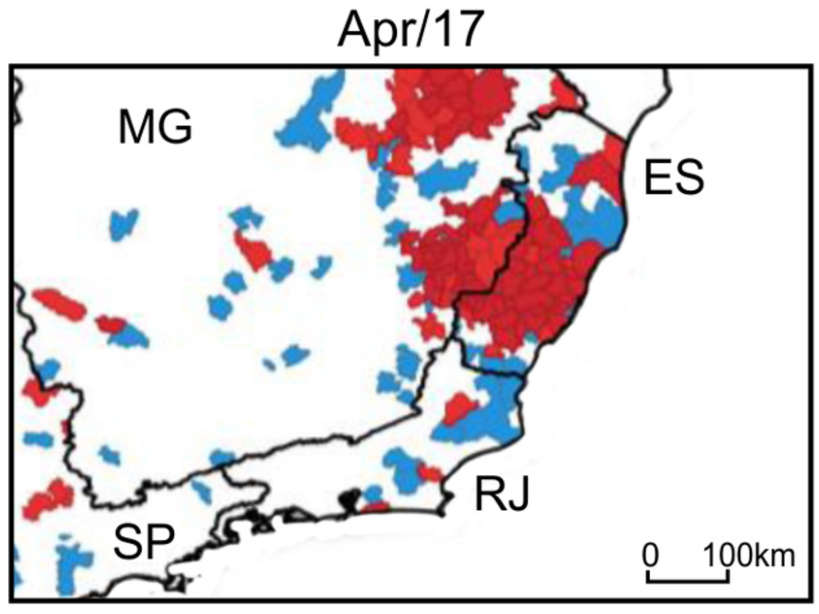

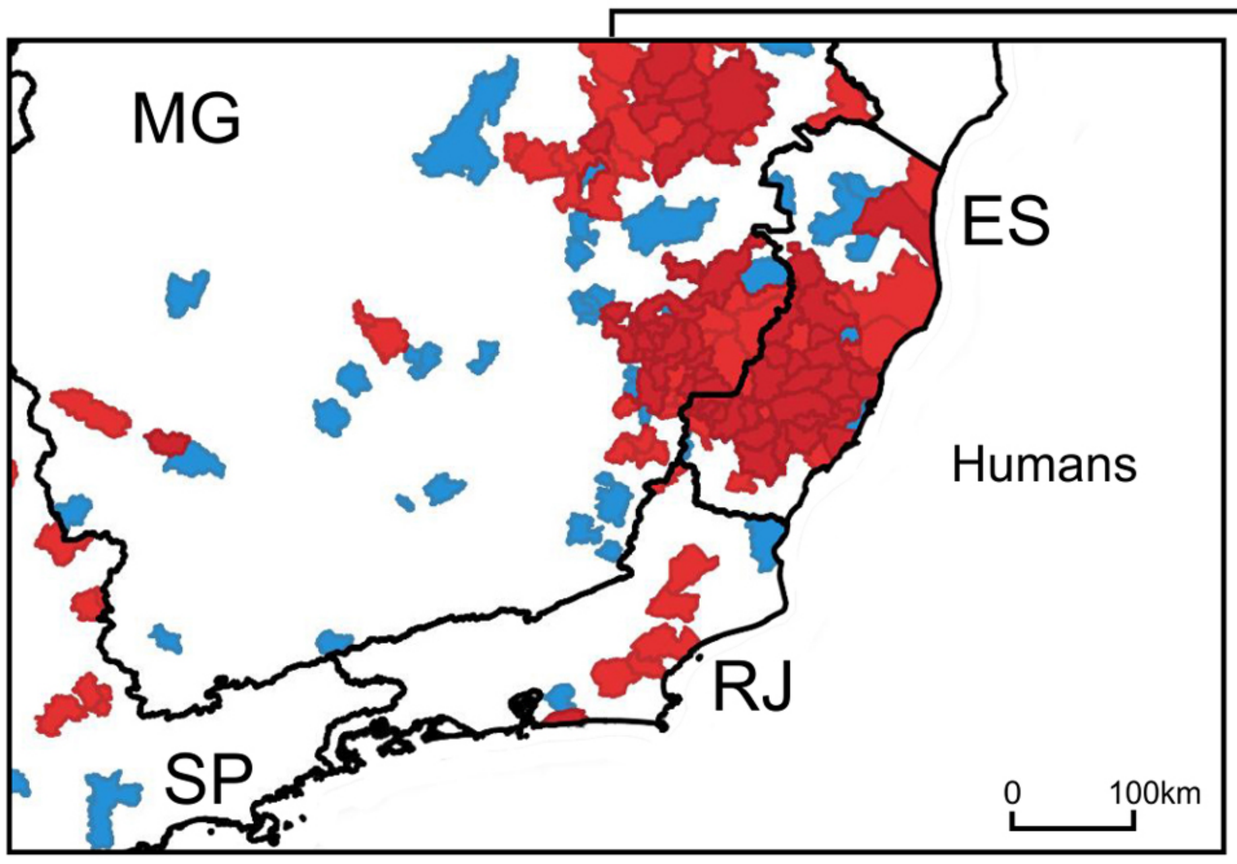

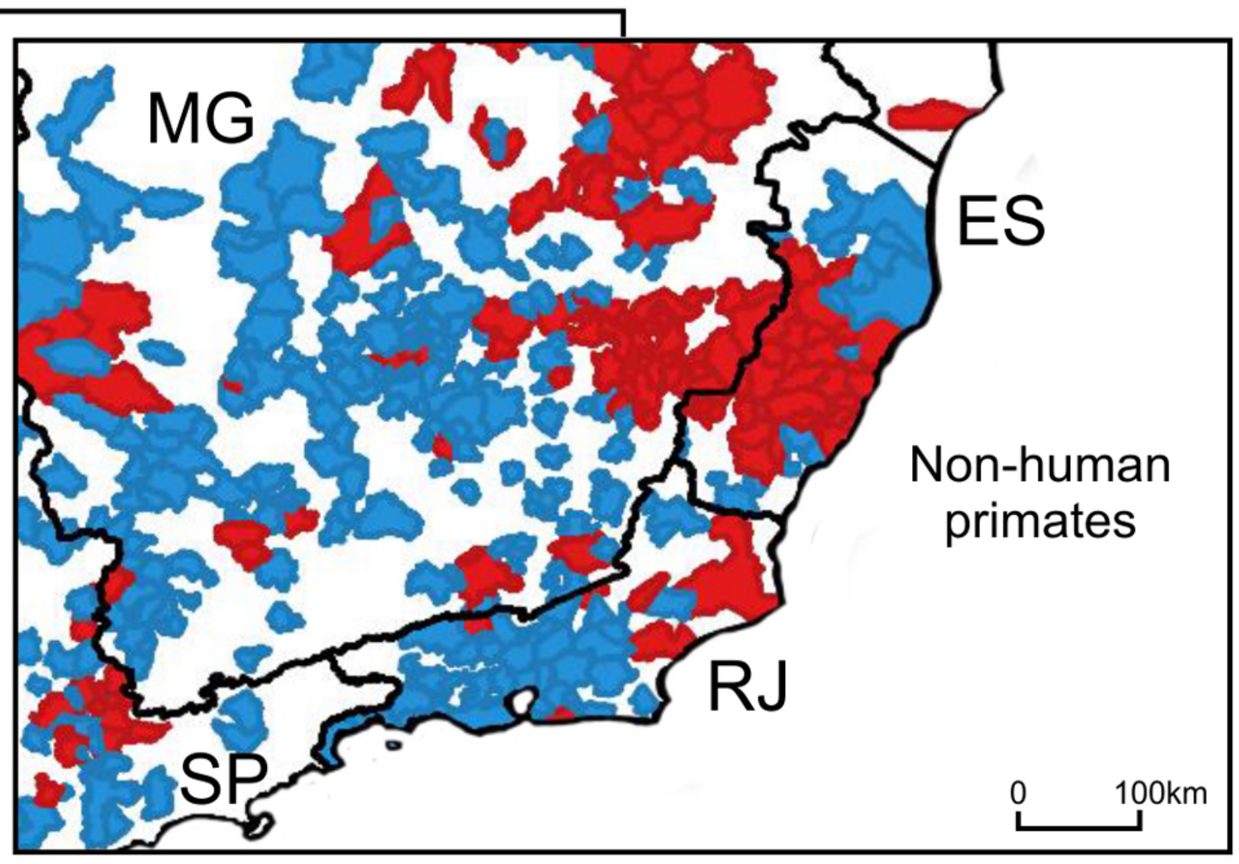

Suspected cases Laboratory confirmed cases

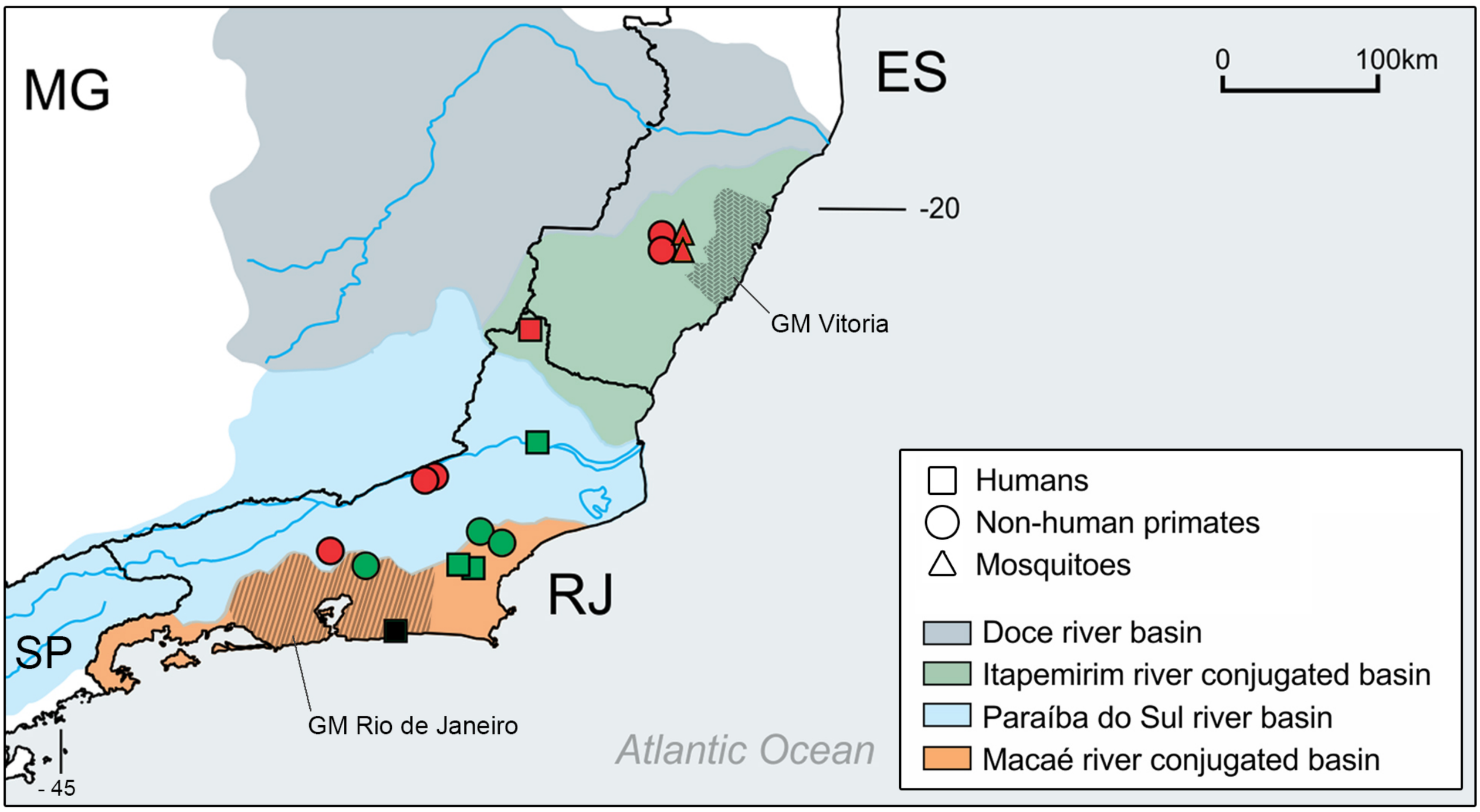

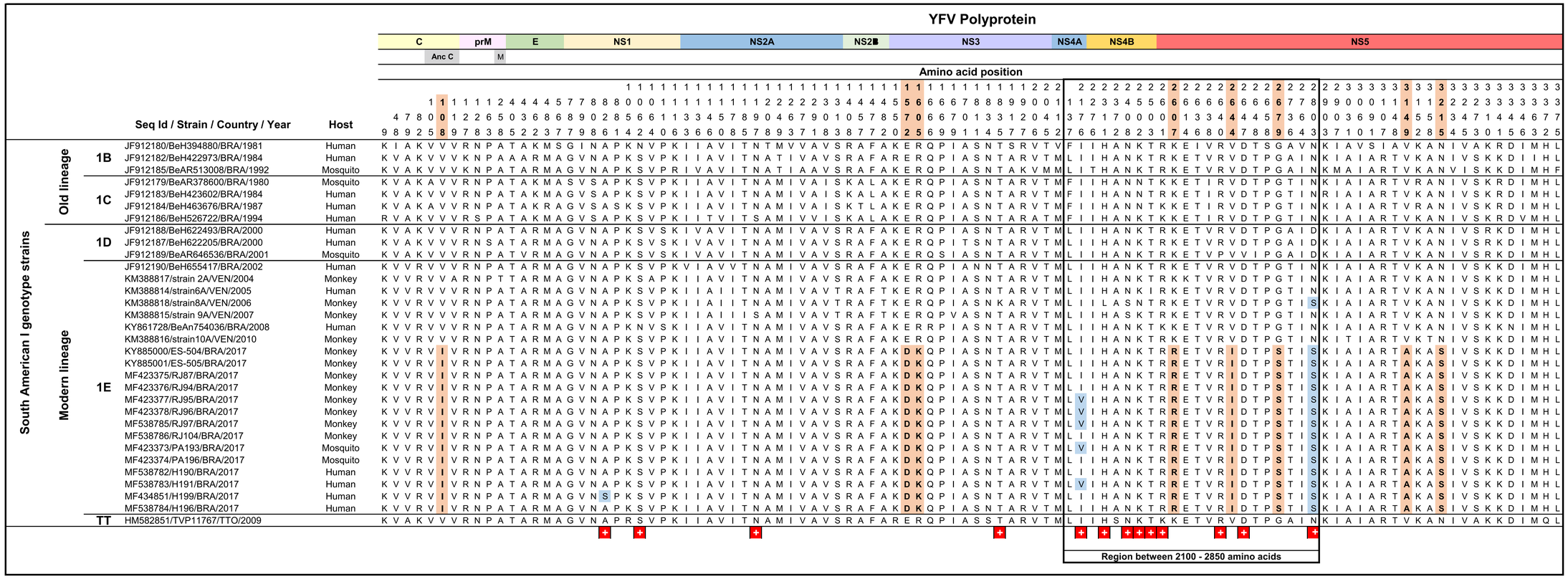
YFV Polyprotein
C
prM
E
NS1
NS2A
NS2B
NS3
NS4A
NS4B
NS5
Anc C
M
Amino acid position
Seq Id / Strain / Country / Year
Host
South American I genotype strains
Old lineage
Modern lineage
1B
1C
1D
1E
TT
JF912180/BeH394880/BRA/1981 Human
JF912182/BeH422973/BRA/1984 Human
JF912185/BeAR513008/BRA/1992 Mosquito
JF912179/BeAR378600/BRA/1980 Mosquito
JF912183/BeH423602/BRA/1984 Human
JF912184/BeH463676/BRA/1987 Human
JF912186/BeH526722/BRA/1994 Human
JF912188/BeH622493/BRA/2000 Human
JF912187/BeH622205/BRA/2000 Human
JF912189/BeAR646536/BRA/2001 Mosquito
JF912190/BeH655417/BRA/2002 Human
KM388817/strain 2A/VEN/2004 Monkey
KM388814/strain6A/VEN/2005 Human
KM388818/strain8A/VEN/2006 Monkey
KM388815/strain 9A/VEN/2007 Monkey
KY861728/BeAn754036/BRA/2008 Human
KM388816/strain10A/VEN/2010 Monkey
KY885000/ES-504/BRA/2017 Monkey
KY885001/ES-505/BRA/2017 Monkey
MF423375/RJ87/BRA/2017 Monkey
MF423376/RJ94/BRA/2017 Monkey
MF423377/RJ95/BRA/2017 Monkey
MF423378/RJ96/BRA/2017 Monkey
MF538785/RJ97/BRA/2017 Monkey
MF538786/RJ104/BRA/2017 Monkey
MF423373/PA193/BRA/2017 Mosquito
MF423374/PA196/BRA/2017 Mosquito
MF538782/H190/BRA/2017 Human
MF538783/H191/BRA/2017 Human
MF434851/H199/BRA/2017 Human
MF538784/H196/BRA/2017 Human
HM582851/TVP11767/TTO/2009
Region between 2100 - 2850 amino acids

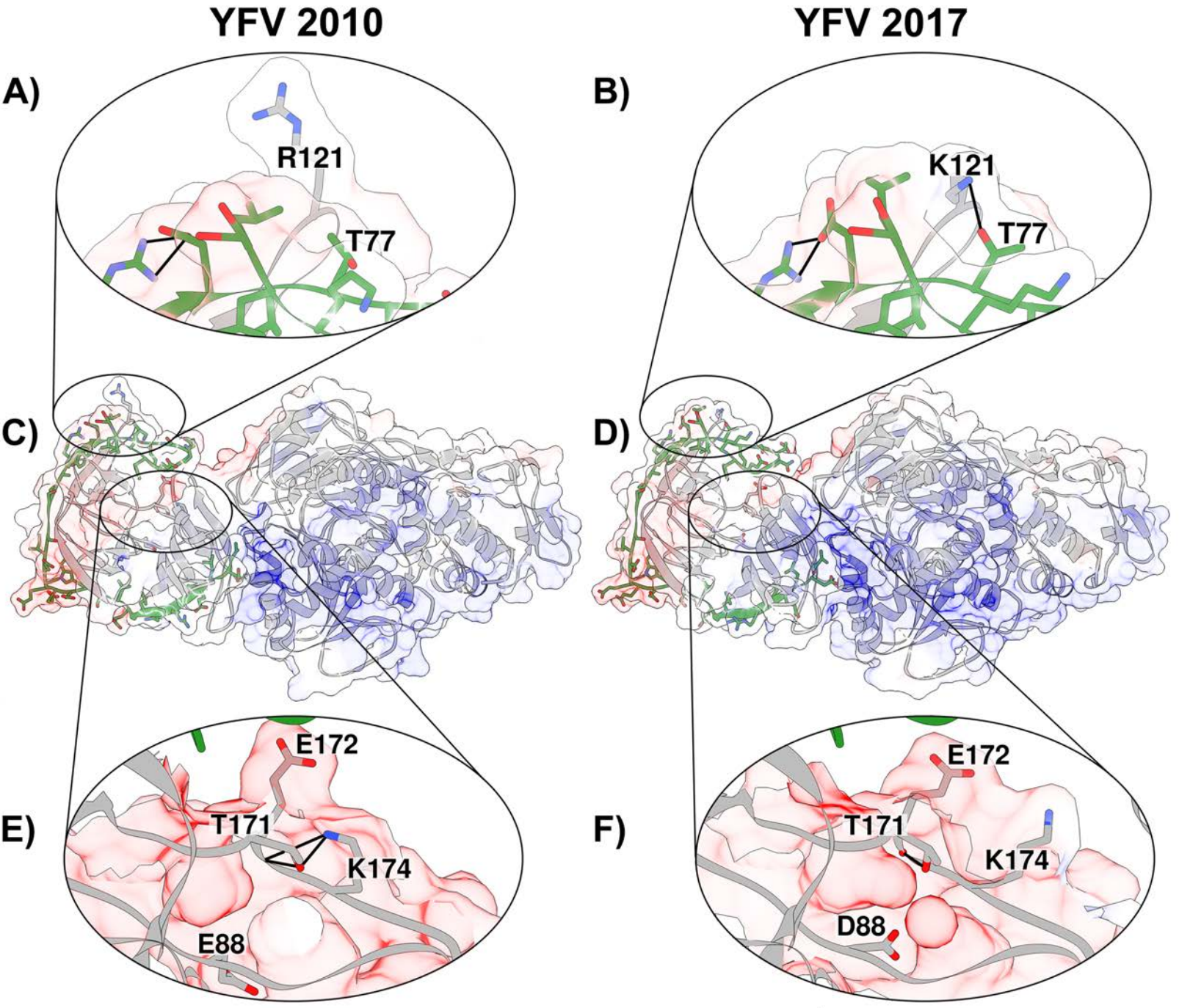
YFV 2010
YFV 2017
A)
B)
R121
T77
K121
T77
C)
D)
E)
F)
E172
T171
K174
E88
E172
T171
K174
D88

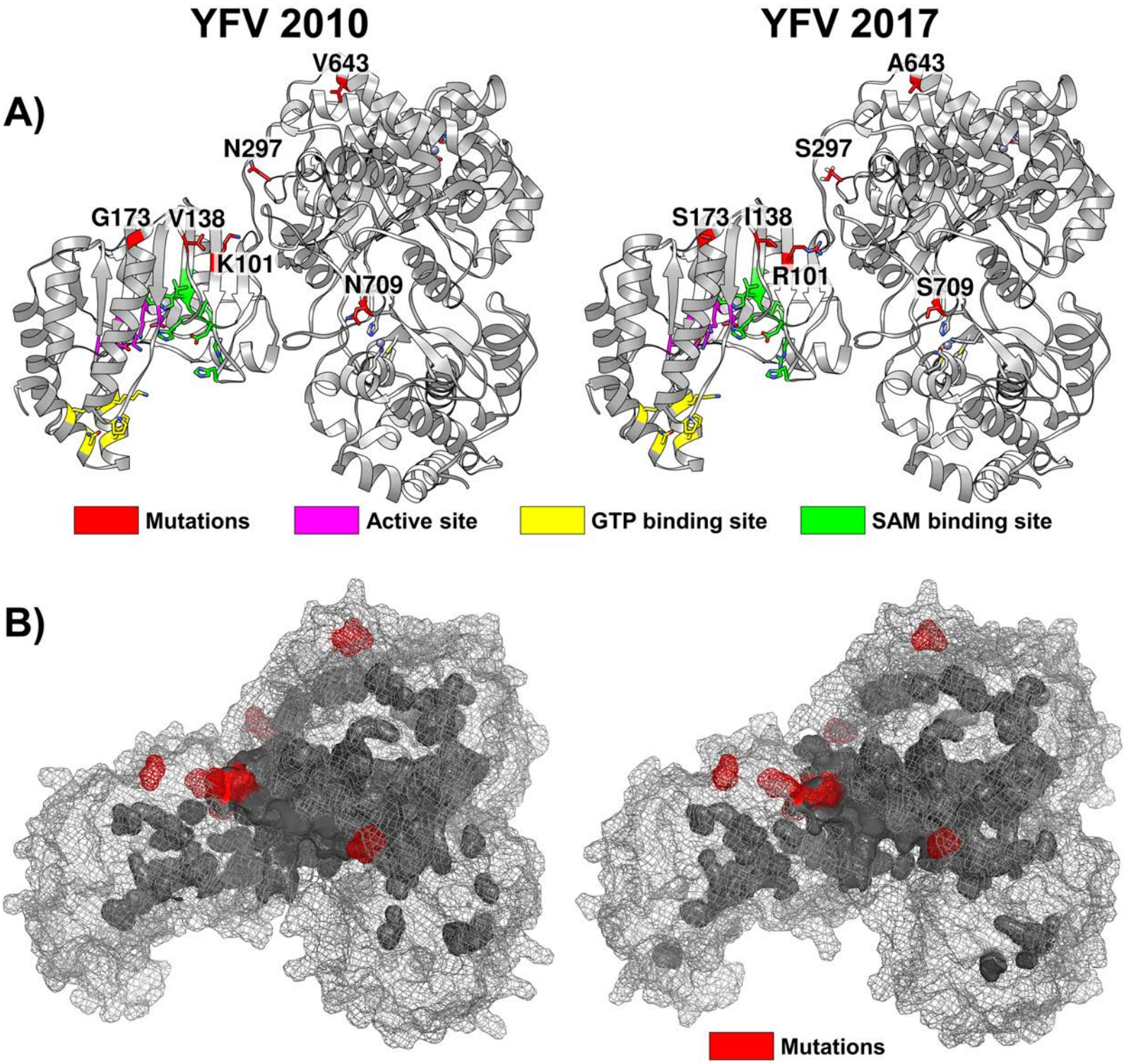
YFV 2010
YFV 2017
A)
V643
N297
G173
V138
K101
N709
A643
S297
S173
I138
R101
S709
Mutations
Active site
GTP binding site
SAM binding site
B)
Mutations

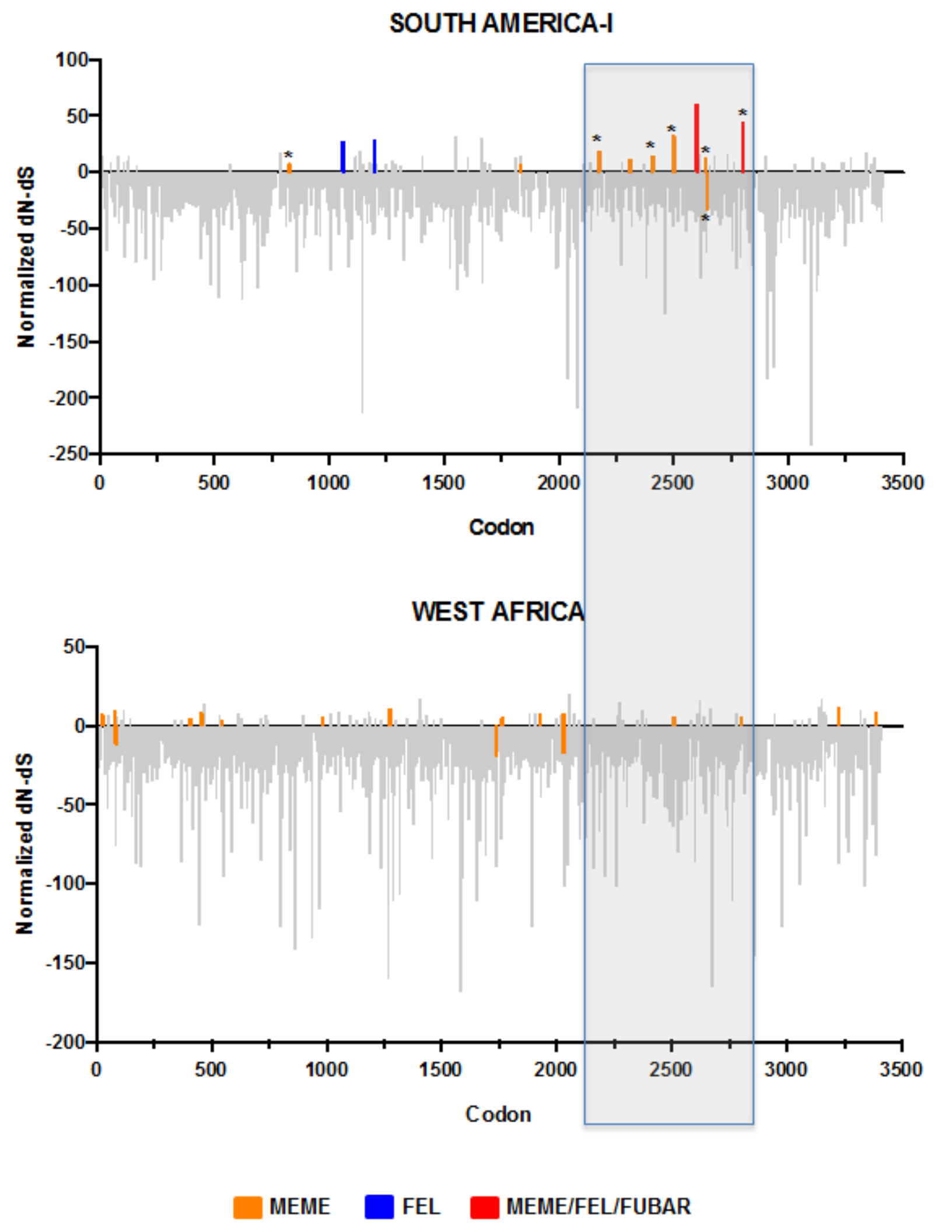
SOUTH AMERICA-I
Normalized dN-dS
100
50
0
-50
-100
-150
-200
-250
0
500
1000
1500
2000
2500
3000
3500
Codon
WEST AFRICA
Normalized dN-dS
50
0
-50
-100
-150
-200
0
500
1000
1500
2000
2500
3000
3500
Codon
MEME
FEL
MEME/FEL/FUBAR

A)

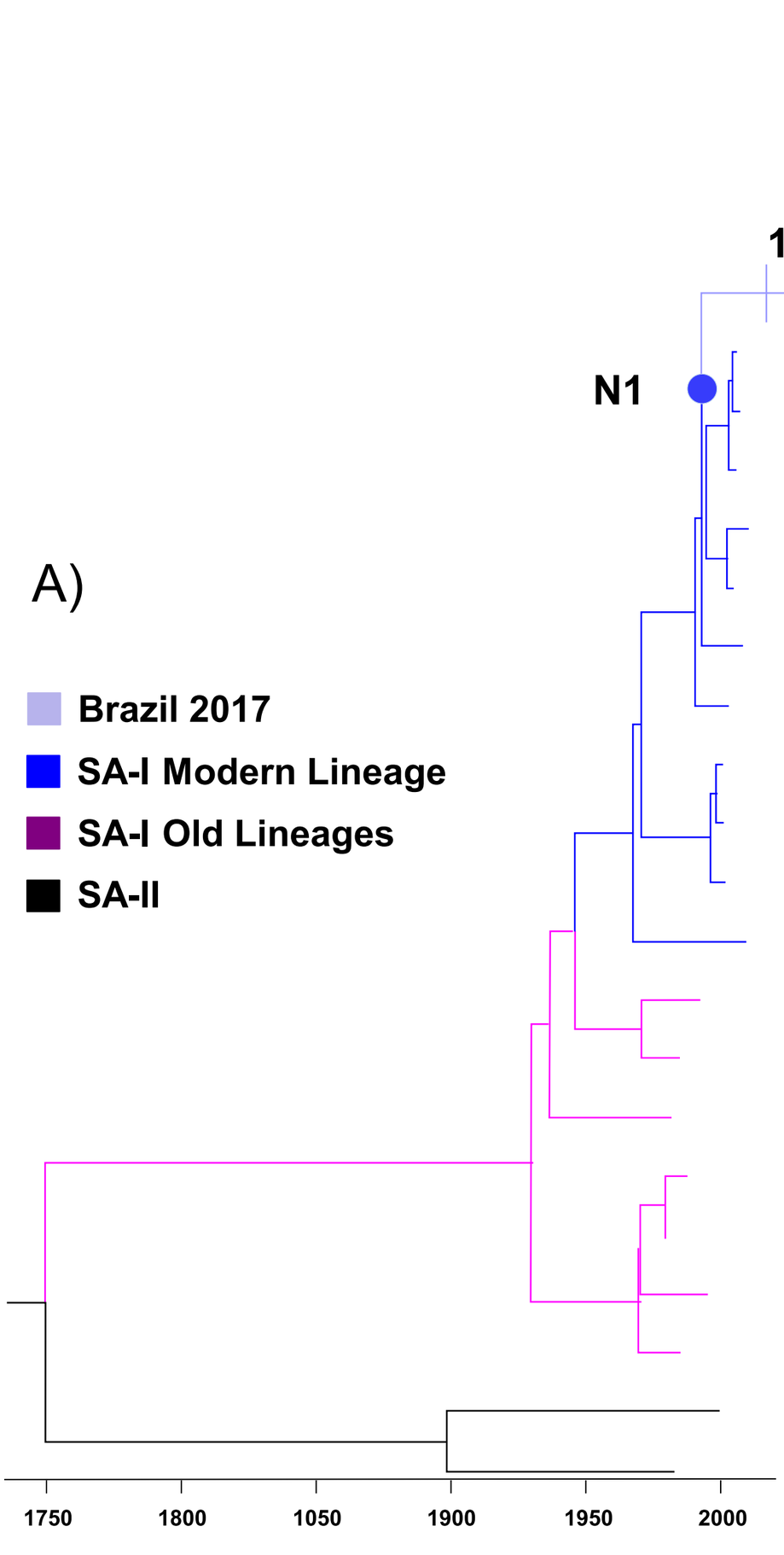

B)

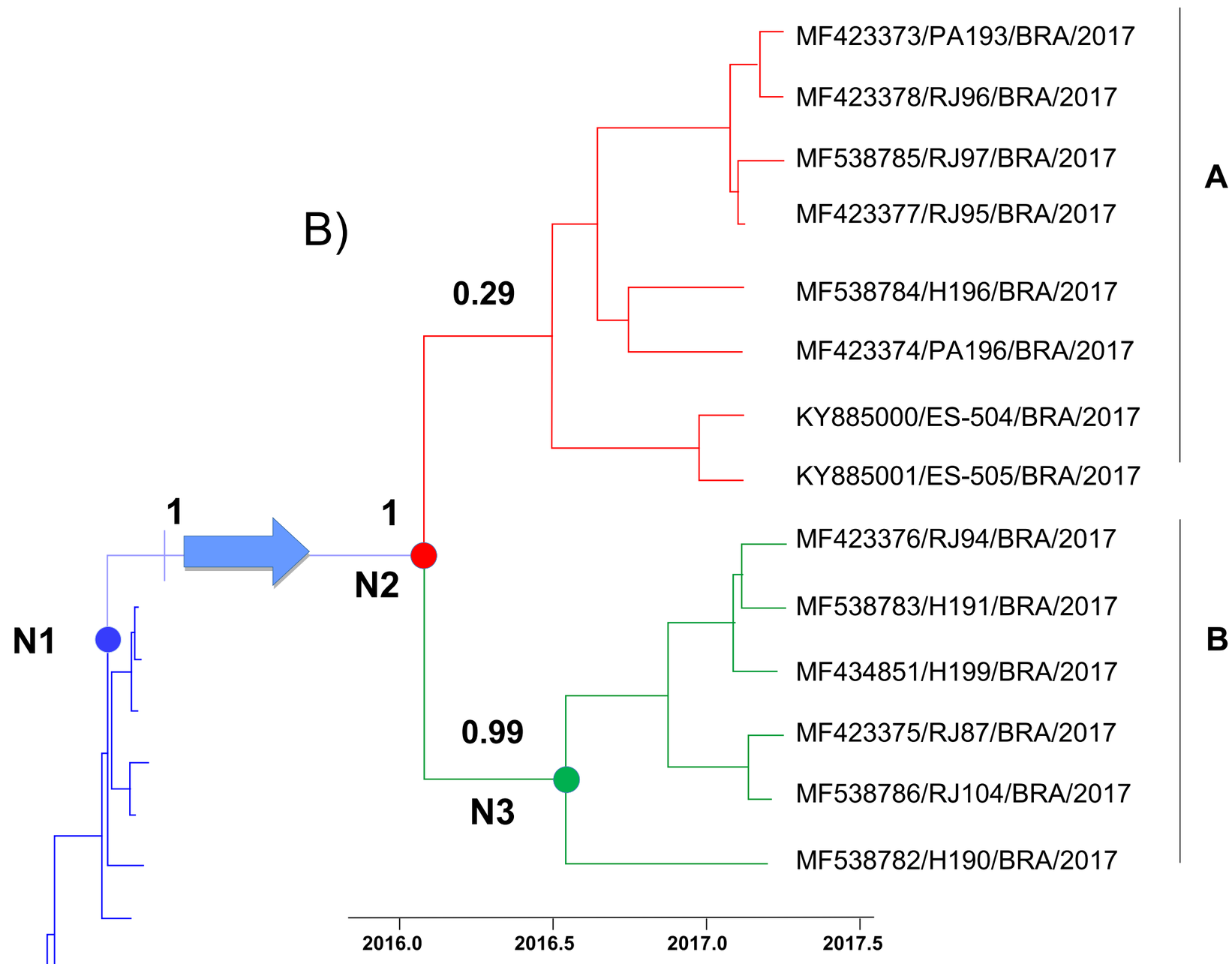

- N1-T_{MRCA} = 1993 (1987 – 1997)
- N2-T_{MRCA} = 2016.3 (2015.6 – 2016.8)
- N3-T_{MRCA} = 2016.8 (2016.3 – 2017.1)

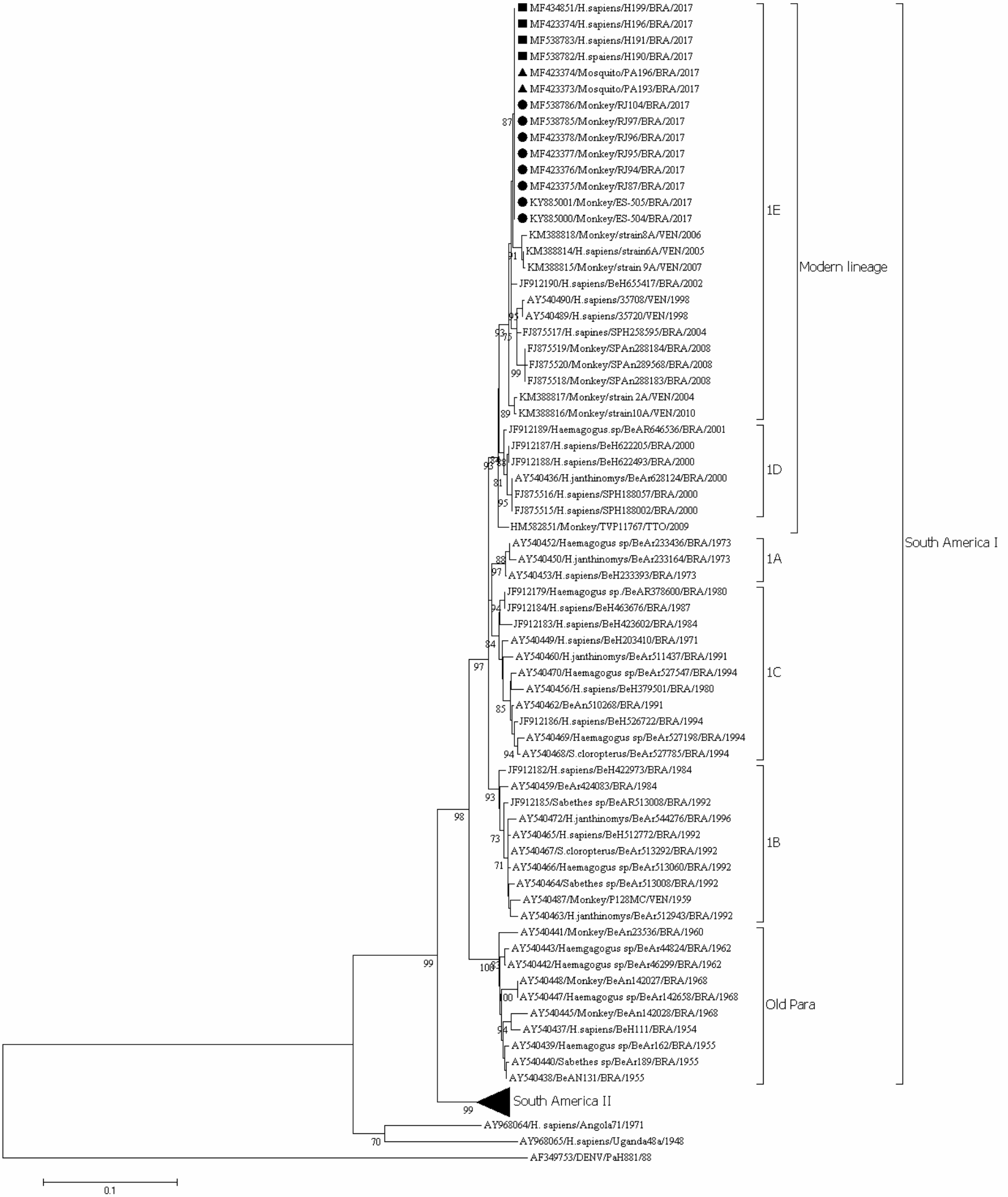
MF434851/H.sapiens/H199/BRA/2017
MF423374/H.sapiens/H196/BRA/2017
MF538783/H.sapiens/H191/BRA/2017
MF538782/H.spaiens/H190/BRA/2017
MF423374/Mosquito/PA196/BRA/2017
MF423373/Mosquito/PA193/BRA/2017
MF538786/Monkey/RJ104/BRA/2017
MF538785/Monkey/RJ97/BRA/2017
MF423378/Monkey/RJ96/BRA/2017
MF423377/Monkey/RJ95/BRA/2017
MF423376/Monkey/RJ94/BRA/2017
MF423375/Monkey/RJ87/BRA/2017
KY885001/Monkey/ES-505/BRA/2017
KY885000/Monkey/ES-504/BRA/2017
KM388818/Monkey/strain8A/VEN/2006
KM388814/H.sapiens/strain6A/VEN/2005
KM388815/Monkey/strain 9A/VEN/2007
JF912190/H.sapiens/BeH655417/BRA/2002
AY540490/H.sapiens/35708/VEN/1998
AY540489/H.sapiens/35720/VEN/1998
FJ875517/H.sapines/SPH258595/BRA/2004
FJ875519/Monkey/SPAn288184/BRA/2008
FJ875520/Monkey/SPAn289568/BRA/2008
FJ875518/Monkey/SPAn288183/BRA/2008
KM388817/Monkey/strain 2A/VEN/2004
KM388816/Monkey/strain10A/VEN/2010
JF912189/Haemagogus.sp/BeAR646536/BRA/2001
JF912187/H.sapiens/BeH622205/BRA/2000
JF912188/H.sapiens/BeH622493/BRA/2000
AY540436/H.janthinomys/BeAr628124/BRA/2000
FJ875516/H.sapiens/SPH188057/BRA/2000
FJ875515/H.sapiens/SPH188002/BRA/2000
HM582851/Monkey/TVP11767/TTO/2009
AY540452/Haemagogus sp/BeAr233436/BRA/1973
AY540450/H.janthinomys/BeAr233164/BRA/1973
AY540453/H.sapiens/BeH233393/BRA/1973
JF912179/Haemagogus sp./BeAR378600/BRA/1980
JF912184/H.sapiens/BeH463676/BRA/1987
JF912183/H.sapiens/BeH423602/BRA/1984
AY540449/H.sapiens/BeH203410/BRA/1971
AY540460/H.janthinomys/BeAr511437/BRA/1991
AY540470/Haemagogus sp/BeAr527547/BRA/1994
AY540456/H.sapiens/BeH379501/BRA/1980
AY540462/BeAn510268/BRA/1991
JF912186/H.sapiens/BeH526722/BRA/1994
AY540469/Haemagogus sp/BeAr527198/BRA/1994
AY540468/S.cloropterus/BeAr527785/BRA/1994
JF912182/H.sapiens/BeH422973/BRA/1984
AY540459/BeAr424083/BRA/1984
JF912185/Sabethes sp/BeAR513008/BRA/1992
AY540472/H.janthinomys/BeAr544276/BRA/1996
AY540465/H.sapiens/BeH512772/BRA/1992
AY540467/S.cloropterus/BeAr513292/BRA/1992
AY540466/Haemagogus sp/BeAr513060/BRA/1992
AY540464/Sabethes sp/BeAr513008/BRA/1992
AY540487/Monkey/P128MC/VEN/1959
AY540463/H.janthinomys/BeAr512943/BRA/1992
AY540441/Monkey/BeAn23536/BRA/1960
AY540443/Haemgagogus sp/BeAr44824/BRA/1962
AY540442/Haemagogus sp/BeAr46299/BRA/1962
AY540448/Monkey/BeAn142027/BRA/1968
AY540447/Haemagogus sp/BeAr142658/BRA/1968
AY540445/Monkey/BeAn142028/BRA/1968
AY540437/H.sapiens/BeH111/BRA/1954
AY540439/Haemagogus sp/BeAr162/BRA/1955
AY540440/Sabethes sp/BeAr189/BRA/1955
AY540438/BeAN131/BRA/1955
South America II
AY968064/H. sapiens/Angola71/1971
AY968065/H.sapiens/Uganda48a/1948
AF349753/DENV/PaH881/88
1E
1D
1A
1C
1B
Old Para
Modern lineage
South America I
0.1

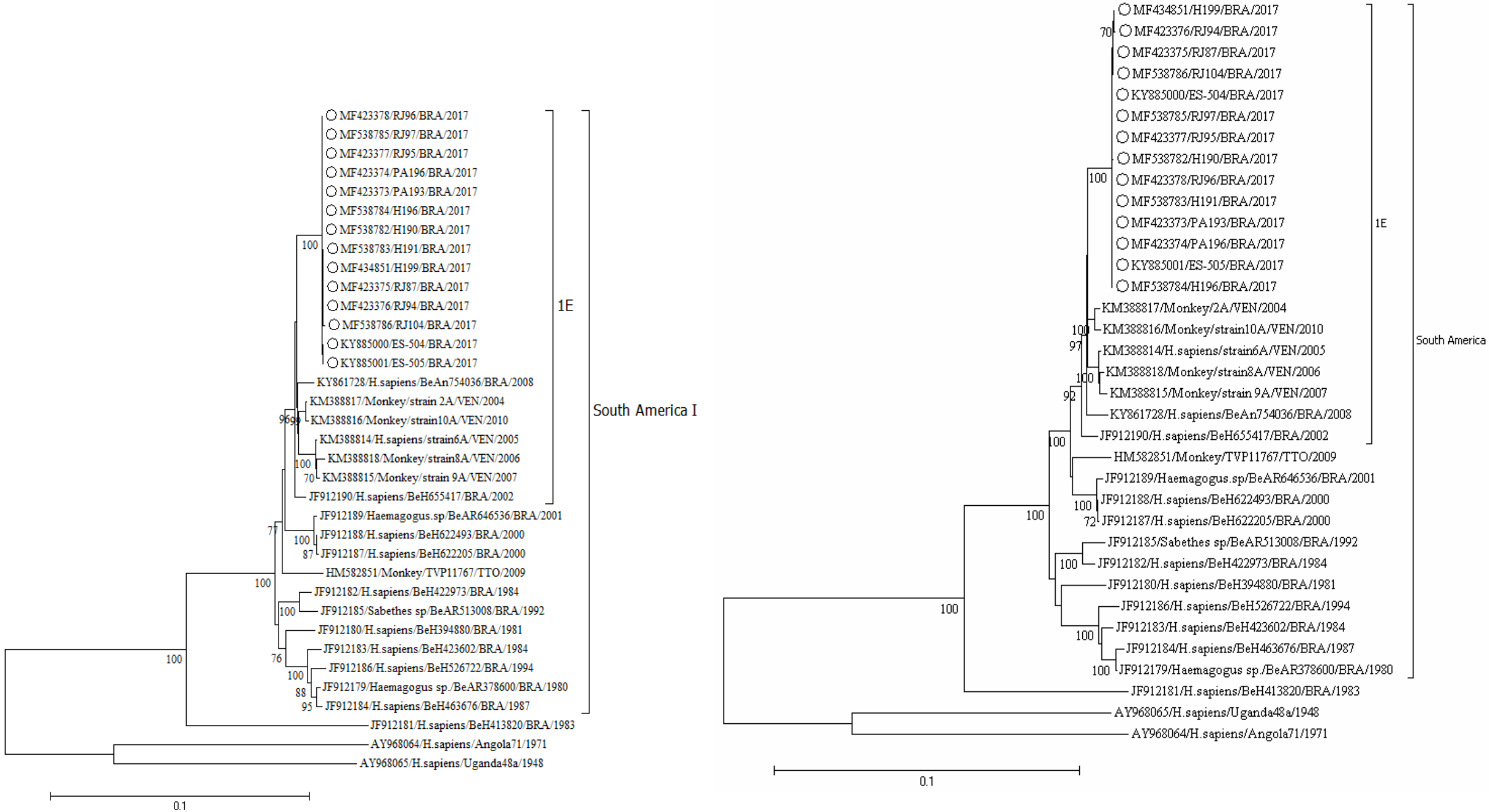
MF423378/RJ96/BRA/2017
MF538785/RJ97/BRA/2017
MF423377/RJ95/BRA/2017
MF423374/PA196/BRA/2017
MF423373/PA193/BRA/2017
MF538784/H196/BRA/2017
MF538782/H190/BRA/2017
MF538783/H191/BRA/2017
MF434851/H199/BRA/2017
MF423375/RJ87/BRA/2017
MF423376/RJ94/BRA/2017
MF538786/RJ104/BRA/2017
KY885000/ES-504/BRA/2017
KY885001/ES-505/BRA/2017
1E
KY861728/H.sapiens/BeAn754036/BRA/2008
KM388817/Monkey/strain 2A/VEN/2004
KM388816/Monkey/strain10A/VEN/2010
KM388814/H.sapiens/strain6A/VEN/2005
KM388818/Monkey/strain8A/VEN/2006
KM388815/Monkey/strain 9A/VEN/2007
JF912190/H.sapiens/BeH655417/BRA/2002
South America I
JF912189/Haemagogus.sp/BeAR646536/BRA/2001
JF912188/H.sapiens/BeH622493/BRA/2000
JF912187/H.sapiens/BeH622205/BRA/2000
HM582851/Monkey/TVP11767/TTO/2009
JF912182/H.sapiens/BeH422973/BRA/1984
JF912185/Sabethes sp/BeAR513008/BRA/1992
JF912180/H.sapiens/BeH394880/BRA/1981
JF912183/H.sapiens/BeH423602/BRA/1984
JF912186/H.sapiens/BeH526722/BRA/1994
JF912179/Haemagogus sp./BeAR378600/BRA/1980
JF912184/H.sapiens/BeH463676/BRA/1987
JF912181/H.sapiens/BeH413820/BRA/1983
AY968064/H.sapiens/Angola71/1971
AY968065/H.sapiens/Uganda48a/1948
0.1
MF434851/H199/BRA/2017
MF423376/RJ94/BRA/2017
MF423375/RJ87/BRA/2017
MF538786/RJ104/BRA/2017
KY885000/ES-504/BRA/2017
MF538785/RJ97/BRA/2017
MF423377/RJ95/BRA/2017
MF538782/H190/BRA/2017
MF423378/RJ96/BRA/2017
MF538783/H191/BRA/2017
MF423373/PA193/BRA/2017
MF423374/PA196/BRA/2017
KY885001/ES-505/BRA/2017
MF538784/H196/BRA/2017
1E
KM388817/Monkey/2A/VEN/2004
KM388816/Monkey/strain10A/VEN/2010
KM388814/H.sapiens/strain6A/VEN/2005
KM388818/Monkey/strain8A/VEN/2006
KM388815/Monkey/strain 9A/VEN/2007
KY861728/H.sapiens/BeAn754036/BRA/2008
JF912190/H.sapiens/BeH655417/BRA/2002
South America I
HM582851/Monkey/TVP11767/TTO/2009
JF912189/Haemagogus.sp/BeAR646536/BRA/2001
JF912188/H.sapiens/BeH622493/BRA/2000
JF912187/H.sapiens/BeH622205/BRA/2000
JF912185/Sabethes sp/BeAR513008/BRA/1992
JF912182/H.sapiens/BeH422973/BRA/1984
JF912180/H.sapiens/BeH394880/BRA/1981
JF912186/H.sapiens/BeH526722/BRA/1994
JF912183/H.sapiens/BeH423602/BRA/1984
JF912184/H.sapiens/BeH463676/BRA/1987
JF912179/Haemagogus sp./BeAR378600/BRA/1980
JF912181/H.sapiens/BeH413820/BRA/1983
AY968065/H.sapiens/Uganda48a/1948
AY968064/H.sapiens/Angola71/1971
0.1

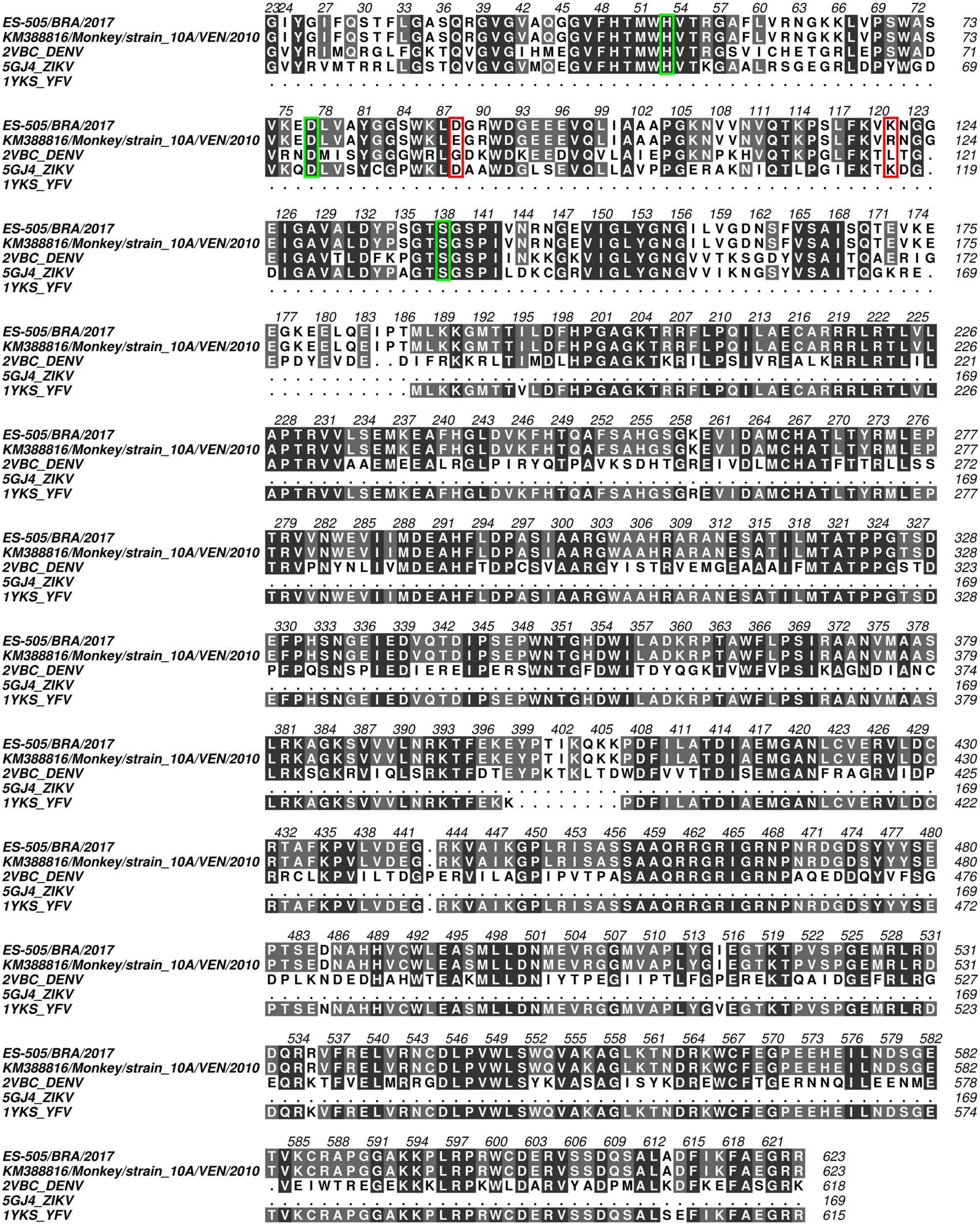

23 24 27 30 33 36 39 42 45 48 51 54 57 60 63 66 69 72
ES-505/BRA/2017 GIYGIFQSTFLGASQRGVGVAQGGVFHTMWHVTRGAFLVRNGKKLVPSWAS 73
KM388816/Monkey/strain_10A/VEN/2010 GIYGIFQSTFLGASQRGVGVAQGGVFHTMWHVTRGAFLVRNGKKLVPSWAS 73
2VBC_DENV GVYRIMQRGLFGKTQVGVGIHMEGVFHTMWHVTRGSVICHETGRLEPSWAD 71
5GJ4_ZIKV GVYRVMTRRLLGSTQVGVGVMQEGVFHTMWHVTKGAALRSGEGRLDPYWGD 69
1YKS_YFV ....
75 78 81 84 87 90 93 96 99 102 105 108 111 114 117 120 123
ES-505/BRA/2017 VKEDLVAYGGSWKLDGRWDGEEEVQLIAAAPGKNVVNVQTKPSLFKVKNGG 124
KM388816/Monkey/strain_10A/VEN/2010 VKEDLVAYGGSWKLEGRWDGEEEVQLIAAAPGKNVVNVQTKPSLFKVRNGG 124
2VBC_DENV VRNDMISYGGGWRLGDKWDKEEDVQVLAIEPGKNPKHVQTKPGLFKTLTG. 121
5GJ4_ZIKV VKQDLVSYCGPWKLDAAWDGLSEVQLLAVPPGERAKNIQTLPGIFKTKDG. 119
1YKS_YFV ....
126 129 132 135 138 141 144 147 150 153 156 159 162 165 168 171 174
ES-505/BRA/2017 EIGAVALDYPSGTSGSPIVNRNGEVIGLYGNGILVGDNSFVSAISQTEVKE 175
KM388816/Monkey/strain_10A/VEN/2010 EIGAVALDYPSGTSGSPIVNRNGEVIGLYGNGILVGDNSFVSAISQTEVKE 175
2VBC_DENV EIGAVTLDFKPGTSGSPIINKKGKVIGLYGNGVVTKSGDYVSAITQAERIG 172
5GJ4_ZIKV DIGAVALDYPAGTSGSPILDKCGRVIGLYGNGVVIKNGSYVSAITQGKRE. 169
1YKS_YFV ....
177 180 183 186 189 192 195 198 201 204 207 210 213 216 219 222 225
ES-505/BRA/2017 EGKEELQEIPTMLKKGMTTILDFHPGAGKTRRFLPQILAECARRRLRTLVL 226
KM388816/Monkey/strain_10A/VEN/2010 EGKEELQEIPTMLKKGMTTILDFHPGAGKTRRFLPQILAECARRRLRTLVL 226
2VBC_DENV EPDYEVDE..DIFRKKRLTIMDLHPGAGKTKRILPSIVREALKRRLRTLIL 221
5GJ4_ZIKV 169
1YKS_YFV ...........MLKKGMTTVLDFHPGAGKTRRFLPQILAECARRRLRTLVL 226
228 231 234 237 240 243 246 249 252 255 258 261 264 267 270 273 276
ES-505/BRA/2017 APTRVVLSEMKEAFHGLDVKFHTQAFSAHGSGKEVIDAMCHATLTYRMLEP 277
KM388816/Monkey/strain_10A/VEN/2010 APTRVVLSEMKEAFHGLDVKFHTQAFSAHGSGKEVIDAMCHATLTYRMLEP 277
2VBC_DENV APTRVVAAEMEEALRGLPIRYQTPAVKSDHTGREIVDLMCHATFTTRLLSS 272
5GJ4_ZIKV 169
1YKS_YFV APTRVVLSEMKEAFHGLDVKFHTQAFSAHGSGREVIDAMCHATLTYRMLEP 277
279 282 285 288 291 294 297 300 303 306 309 312 315 318 321 324 327
ES-505/BRA/2017 TRVVNWEVIIMDEAHFLDPASIAARGWAAHRARANESATILMTATPPGTSD 328
KM388816/Monkey/strain_10A/VEN/2010 TRVVNWEVIIMDEAHFLDPASIAARGWAAHRARANESATILMTATPPGTSD 328
2VBC_DENV TRVPNYNLIVMDEAHFTDPCSVAARGYISTRVEMGEAAAIFMTATPPGSTD 323
5GJ4_ZIKV 169
1YKS_YFV TRVVNWEVIIMDEAHFLDPASIAARGWAAHRARANESATILMTATPPGTSD 328
330 333 336 339 342 345 348 351 354 357 360 363 366 369 372 375 378
ES-505/BRA/2017 EFPHSNGEIEDVQTDIPSEPWNTGHDWILADKRPTAWFLPSIRAANVMAAS 379
KM388816/Monkey/strain_10A/VEN/2010 EFPHSNGEIEDVQTDIPSEPWNTGHDWILADKRPTAWFLPSIRAANVMAAS 379
2VBC_DENV PFPQSNSPIEDIEREIPERSWNTGFDWITDYQGKTVWFVPSIKAGNDIANC 374
5GJ4_ZIKV 169
1YKS_YFV EFPHSNGEIEDVQTDIPSEPWNTGHDWILADKRPTAWFLPSIRAANVMAAS 379
381 384 387 390 393 396 399 402 405 408 411 414 417 420 423 426 429
ES-505/BRA/2017 LRKAGKSVVVLNRKTFEKEYPTIKQKKPDFILATDIAEMGANLCVERVLDC 430
KM388816/Monkey/strain_10A/VEN/2010 LRKAGKSVVVLNRKTFEKEYPTIKQKKPDFILATDIAEMGANLCVERVLDC 430
2VBC_DENV LRKSGKRVIQLSRKTFDTEYPKTKLTDWDFVVTTDISEMGANFRAGRVIDP 425
5GJ4_ZIKV 169
1YKS_YFV LRKAGKSVVVLNRKTFEKK........PDFILATDIAEMGANLCVERVLDC 422
432 435 438 441 444 447 450 453 456 459 462 465 468 471 474 477 480
ES-505/BRA/2017 RTAFKPVLVDEG.RKVAIKGPLRISASSAAQRRGRIGRNPNRDGDSYYYSE 480
KM388816/Monkey/strain_10A/VEN/2010 RTAFKPVLVDEG.RKVAIKGPLRISASSAAQRRGRIGRNPNRDGDSYYYSE 480
2VBC_DENV RRCLKPVILTDGPERVILAGPIPVTPASAAQRRGRIGRNPAQEDDQYVFSG 476
5GJ4_ZIKV 169
1YKS_YFV RTAFKPVLVDEG.RKVAIKGPLRISASSAAQRRGRIGRNPNRDGDSYYYSE 472
483 486 489 492 495 498 501 504 507 510 513 516 519 522 525 528 531
ES-505/BRA/2017 PTSEDNAHHVCWLEASMLLDNMEVRGGMVAPLYGIEGTKTPVSPGEMRLRD 531
KM388816/Monkey/strain_10A/VEN/2010 PTSEDNAHHVCWLEASMLLDNMEVRGGMVAPLYGIEGTKTPVSPGEMRLRD 531
2VBC_DENV DPLKNDEDHAHWTEAKMLLDNIYTPEGIIPTLFGPEREKTQAIDGEFRLRG 527
5GJ4_ZIKV 169
1YKS_YFV PTSENNAHHVCWLEASMLLDNMEVRGGMVAPLYGVEGTKTPVSPGEMRLRD 523
534 537 540 543 546 549 552 555 558 561 564 567 570 573 576 579 582
ES-505/BRA/2017 DQRRVFRELVRNCDLPVWLSWQVAKAGLKTNDRKWCFEGPEEHEILNDSGE 582
KM388816/Monkey/strain_10A/VEN/2010 DQRRVFRELVRNCDLPVWLSWQVAKAGLKTNDRKWCFEGPEEHEILNDSGE 582
2VBC_DENV EQRKTFVELMRRGDLPVWLSYKVASAGISYKDREWCFTGERNNQILEENME 578
5GJ4_ZIKV 169
1YKS_YFV DQRKVFRELVRNCDLPVWLSWQVAKAGLKTNDRKWCFEGPEEHEILNDSGE 574
585 588 591 594 597 600 603 606 609 612 615 618 621
ES-505/BRA/2017 TVKCRAPGGAKKPLRPRWCDERVSSDQSALADFIKFAEGRR 623
KM388816/Monkey/strain_10A/VEN/2010 TVKCRAPGGAKKPLRPRWCDERVSSDQSALADFIKFAEGRR 623
2VBC_DENV .VEIWTREGEKKKLRPKWLDARVYADPMALKDFKEFASGRK 618
5GJ4_ZIKV 169
1YKS_YFV TVKCRAPGGAKKPLRPRWCDERVSSDQSALSEFIKFAEGRR 615

```
                                5 6   9   12  15  18  21  24  27  30  33  36  39  42  45  48  51  54  57  60
ES-505/BRA/2017                 G K T L G E V W K R E L N L L D K Q Q F E L Y K R T D I V E V D R D T A R R H L A E G K V D T G V A V S R G T A  60
KM388816/Monkey/strain_10A/VEN/2010 G K T L G E V W K R E L N L L D K Q Q F E L Y K R T D I V E V D R D T A R R H L A E G K V D T G V A V S R G T A  60
4K6M_JEV                        G R T L G E Q W K E K L N A M S R E E F F K Y R R E A I I E V D R T E A R R A R R E N N I V G G H P V S R G S A  60

                                63  66  69  72  75  78  81  84  87  90  93  96  99  102 105 108 111 114
ES-505/BRA/2017                 K L R W F H E R G Y V K L E G R V T D L G C G R G G W C Y Y A A A Q R E V S G V R G F T L G K E G H E K P M N V  116
KM388816/Monkey/strain_10A/VEN/2010 K L R W F H E R G Y V K L E G R V T D L G C G R G G W C Y Y A A A Q R E V S G V K G F T L G K E G H E K P M N V  116
4K6M_JEV                        K L R W L V E K G F V S P I G K V I D L G C G R G G W S Y Y A A T L K K V Q E V R G Y T K G G A G H E E P M L M  116

                                117 120 123 126 129 132 135 138 141 144 147 150 153 156 159 162 165 168 171
ES-505/BRA/2017                 Q S L G W N I I T F K D K T D V H R L E P I K C D T L L C D I G E S S P S S V T E G E R T M R V L D T V E K W L  172
KM388816/Monkey/strain_10A/VEN/2010 Q S L G W N I I T F K D K T D V H R L E P V K C D T L L C D I G E S S P S S V T E G E R T M R V L D T V E K W L  172
4K6M_JEV                        Q S Y G W N L V S L K S G V D V F Y K P S E P S D T L F C D I G E S S P S P E V E E Q R T L R V L E M T S D W L  172

                                174 177 180 183 186 189 192 195 198 201 204 207 210 213 216 219 222 225 228
ES-505/BRA/2017                 S C G V E S F C V K V L A P Y M P D V L E K L E L L Q R R F G G T V I R N P L S R N S T H E M Y Y V S G A R S N  228
KM388816/Monkey/strain_10A/VEN/2010 G C G V E S F C V K V L A P Y M P D V L E K L E L L Q R R F G G T V I R N P L S R N S T H E M Y Y V S G A R S N  228
4K6M_JEV                        H R G P R E F C I K V L C P Y M P K V I E K M E V L Q R R F G G G L V R L P L S R N S N H E M Y W V S G A A G N  228

                                231 234 237 240 243 246 249     252 255 258 261 264 267 270 273 276 279 282
ES-505/BRA/2017                 I T F T V N Q T S R L L M R R M R R P T G K .   V T L E A D V I L P I G T R S V E T D K G P L D R A A I E E R V E  283
KM388816/Monkey/strain_10A/VEN/2010 I T F T V N Q T S R L L M R R M R R P T G K .   V T L E A D V I L P I G T R S V E T D K G P L D R A A I E E R V E  283
4K6M_JEV                        V V H A V N M T S Q V L L G R M D R T V W R G P K Y E E D V N L G S G T R A V G K . . .   G S N Q E K I K K R I Q  281

                                285 288 291 294 297 300 303 306 309 312 315 318 321 324 327 330 333 336 339
ES-505/BRA/2017                 R I K S E Y T A T W F H D S D N P Y R T W H Y C G S Y V T R T S G S A A S M I N G V I K I L T Y P W D R I E E V  339
KM388816/Monkey/strain_10A/VEN/2010 R I K S E Y T A T W F H D N D N P Y R T W H Y C G S Y V T R T S G S A A S M I N G V I K I L T Y P W D R I E E V  339
4K6M_JEV                        K L K E E F A T T W H K D P E H P Y R T W T Y H G S Y E V K A T G S A S S L V N G V V K L M S K P W D A I A N V  337

                                342 345 348 351 354 357 360 363 366 369 372 375 378 381 384 387 390 393
ES-505/BRA/2017                 T R M A M T D T T P F G Q Q R V F K E K V D T R A K D P P A G T R K I M K V V N R W L F R H L A R E K N P R L C  395
KM388816/Monkey/strain_10A/VEN/2010 T R M A M T D T T P F G Q Q R V F K E K V D T R A K D P P A G T R K I M K V V N R W L F R H L A R E K N P R L C  395
4K6M_JEV                        T T M A M T D T T P F G Q Q R V F K E K V D T K A P E P P A G A K E V L N E T T N W L W A Y L S R E K R P R L C  393

                                396 399 402 405 408 411 414 417 420 423 426 429 432 435 438 441 444 447 450
ES-505/BRA/2017                 T K E E F I A K V R S H A A I G A F L E E Q E Q W K T A N E A V Q D P K F W E L V D E E R R L H Q Q G R C R T C  451
KM388816/Monkey/strain_10A/VEN/2010 T K E E F I A K V R S H A A I G A F L E E Q E Q W K T A N E A V Q D P K F W E L V D E E R R L H Q Q G R C R T C  451
4K6M_JEV                        T K E E F I K K V N S N A A L G A V F A E Q N Q W S T A R E A V D D P R F W E M V D E E R E N H L R G E C H T C  449

                                453 456 459 462 465 468 471 474 477 480 483 486 489 492 495 498 501 504 507
ES-505/BRA/2017                 V Y N M M G K R E K K L S E F G K A K G S R A I W Y M W L G A R Y L E F E A L G F L N E D H W A S R E N S G G G  507
KM388816/Monkey/strain_10A/VEN/2010 V Y N M M G K R E K K L S E F G K A K G S R A I W Y M W L G A R Y L E F E A L G F L N E D H W A S R E N S G G G  507
4K6M_JEV                        I Y N M M G K R E K K P G E F G K A K G S R A I W F M W L G A R Y L E F E A L G F L N E D H W L S R E N S G G G  505

                                510 513 516 519 522 525 528 531 534 537 540 543 546 549 552 555 558 561
ES-505/BRA/2017                 V E G I G L Q Y L G Y V I R D L A A L E G G G F Y A D D T A G W D T R I T E A D L D D E Q E I L N Y M S P H H R  563
KM388816/Monkey/strain_10A/VEN/2010 V E G I G L Q Y L G Y V I R D L A T L E G G G F Y A D D T A G W D T R I T E A D L D D E Q E I L N Y M S P H H R  563
4K6M_JEV                        V E G S G V Q K L G Y I L R D I A G K Q G G K M Y A D D T A G W D T R I T R T D L E N E A K V L E L L D G E H R  561

                                564 567 570 573 576 579 582 585 588 591 594 597 600 603 606 609 612 615 618
ES-505/BRA/2017                 K L A L A V M E M T Y K N K V V K V L R P A P G G K A Y M D V I S R R D Q R G S G Q V V T Y A L N T I T N L K V  619
KM388816/Monkey/strain_10A/VEN/2010 K L A L A V M E M T Y K N K V V K V L R P A P G G K A Y M D V I S R R D Q R G S G Q V V T Y A L N T I T N L K V  619
4K6M_JEV                        M L A R A I I E L T Y R H K V V K V M R P A A E G K T V M D V I S R E D Q R G S G Q V V T Y A L N T F T N I A V  617

                                621 624 627 630 633 636 639 642 645 648 651 654 657 660 663 666 669 672 675
ES-505/BRA/2017                 Q L I R M A E A E M V I H H Q H V Q D C D D T A L T K L E A W L A E H G C D R L K R M A V S G D D C V V R P I D  675
KM388816/Monkey/strain_10A/VEN/2010 Q L I R M A E A E M V I H H Q H V Q D C D D T V L T K L E A W L T E H G C D R L K R M A V S G D D C V V R P I D  675
4K6M_JEV                        Q L V R L M E A E G V I G P Q H L E Q L P R K N K I A V R T W L F E N G E E R V T R M A I S G D D C V V K P L D  673

                                678 681 684 687 690 693 696 699 702 705 708 711 714 717 720 723 726 729
ES-505/BRA/2017                 D R F G L A L S H L N A M S K V R K D I S E W Q P S K G W D D W E S V P F C S H H F H E L Q L K D G R R I V V P  731
KM388816/Monkey/strain_10A/VEN/2010 D R F G L A L S H L N A M S K V R K D I S E W Q P S K G W D D W E N V P F C S H H F H E L Q L K D G R R I V V P  731
4K6M_JEV                        D R F A T A L H F L N A M S K V R K D I Q E W K P S H G W H D W Q Q V P F C S N H F Q E I V M K D G R S I V V P  729

                                732 735 738 741 744 747 750 753 756 759 762 765 768 771 774 777 780 783 786
ES-505/BRA/2017                 C R D Q D E L V G R G R V S P G N G W M I K E T A C L S K A Y A N M W S L M Y F H K R D M R L L S L A V S S A V  787
KM388816/Monkey/strain_10A/VEN/2010 C R D Q D E L V G R G R V S P G N G W M I K E T A C L S K A Y A N M W S L M Y F H K R D M R L L S L A V S S A V  787
4K6M_JEV                        C R G Q D E L I G R A R I S P G A G W N V K D T A C L A K A Y A Q M W L L L Y F H R R D L R L M A N A I C S A V  785

                                789 792 795 798 801 804 807 810 813 816 819 822 825 828 831 834 837 840 843
ES-505/BRA/2017                 P T S W V P Q G R T T W S V H G K G E W M T T E D M L E V W N R V W I T N N P H M Q D K T T V K E W R D I P Y L  843
KM388816/Monkey/strain_10A/VEN/2010 P T S W V P Q G R T T W S V H G K G E W M T T E D M L E V W N R V W I T N N P H M Q D K T T V K E W R D I P Y L  843
4K6M_JEV                        P V D W V P T G R T S W S I H S K G E W M T T E D M L Q V W N R V W I E E N E W M M D K T P I T S W T D V P Y V  841

                                846 849 852 855 858 861 864 867 870 873 876 879 882 885 888 891 894
ES-505/BRA/2017                 T K R Q D K L C G S L I G M T N R A T W A S H I H L V I H R I R T L I G K E R Y T D Y L T V M D R Y S  894
KM388816/Monkey/strain_10A/VEN/2010 T K R Q D K L C G S L I G M T N R A T W A S H I H L V I H R I R T L I G K E R Y T D Y L T V M D R Y S  894
4K6M_JEV                        G K R E D I W C G S L I G T R S R A T W A E N I Y A A I N Q V R A V I G K E N Y V D Y M T S L R R Y E  892
```

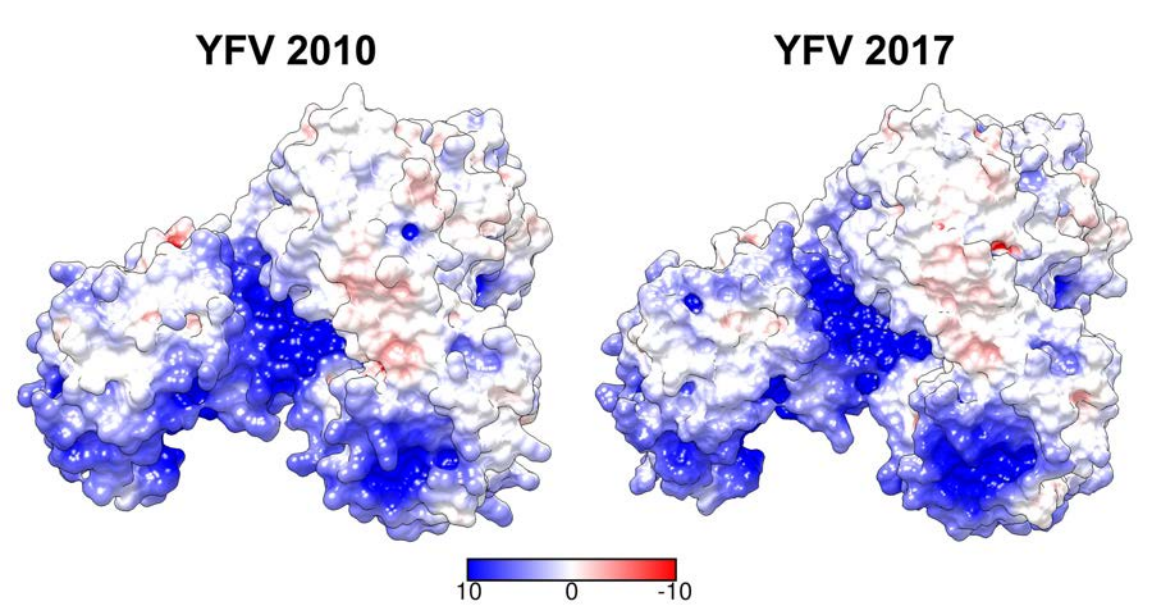
YFV 2010
YFV 2017
10
0
-10

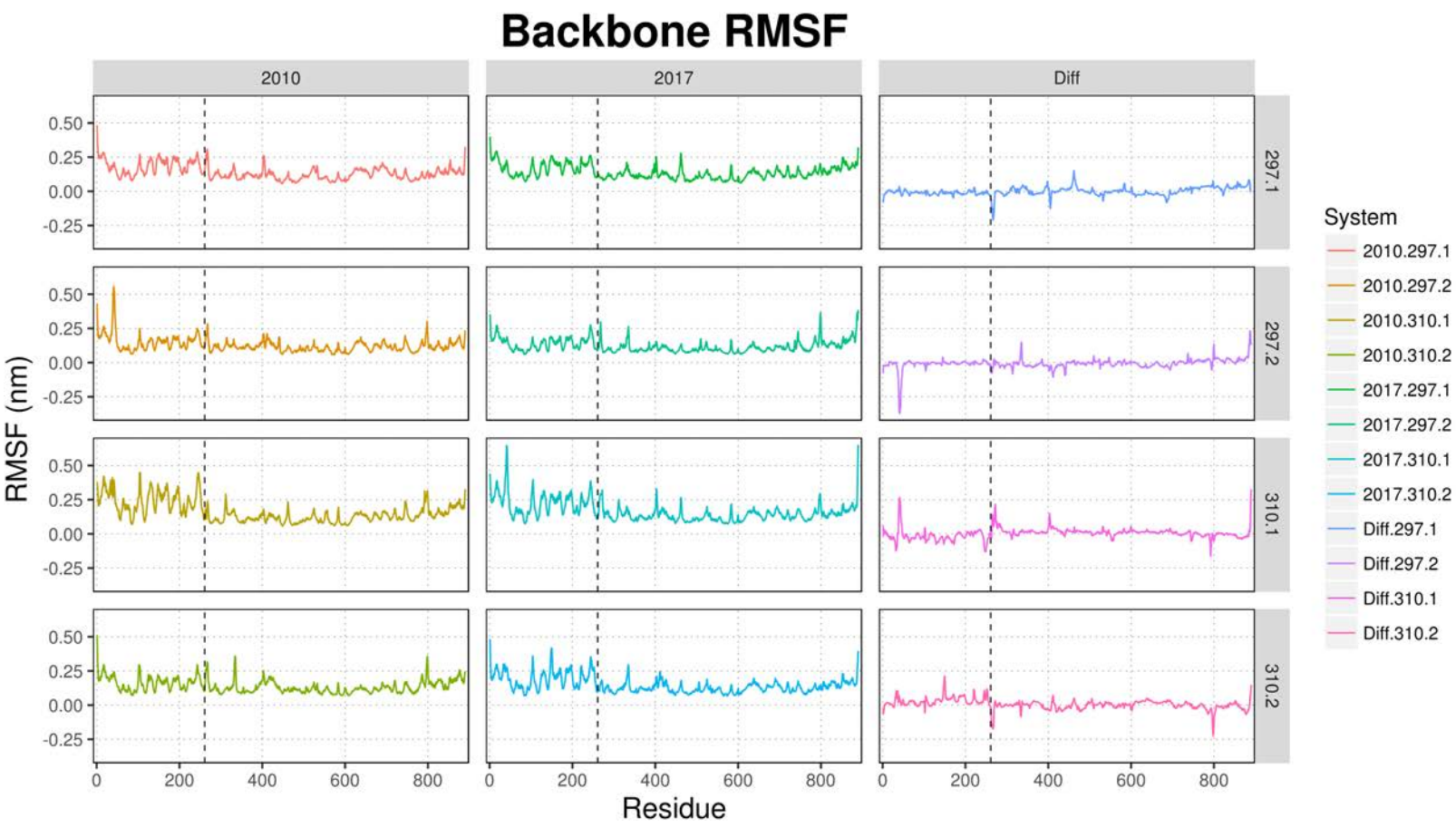
Backbone RMSF
2010
2017
Diff
297.1
297.2
310.1
310.2
RMSF (nm)
0.50
0.25
0.00
-0.25
0
200
400
600
800
Residue
System
2010.297.1
2010.297.2
2010.310.1
2010.310.2
2017.297.1
2017.297.2
2017.310.1
2017.310.2
Diff.297.1
Diff.297.2
Diff.310.1
Diff.310.2

		Seq Id / Strain / Country / Year	NS1		NS2A	NS3	NS4A	NS4B				NS5			
			826[a]	1062[a]	1197[a]	1835[a]	2176[a]	2311[a]	2408[a]	2502[a]	2503[a]	2601[c]	2640[a]	2647[a]	2803[b]
South America genotype I	Old lineage	JF912180/BeH394880/BRA/1981	A	N	N	T	I	H	N	K	T	R	R	D	N
	1B	JF912182/BeH422973/BRA/1984	A	S	N	T	I	H	N	K	T	R	R	D	N
		JF912185/BeAR513008/BRA/1992	A	S	N	T	I	H	N	K	T	R	R	D	N
	1C	JF912179/BeAR378600/BRA/1980	A	S	N	T	I	H	N	N	T	K	R	D	N
		JF912183/BeH423602/BRA/1984	A	S	N	T	I	H	N	N	T	R	R	D	N
		JF912184/BeH463676/BRA/1987	A	S	N	T	I	H	N	N	T	K	R	D	N
		JF912186/BeH526722/BRA/1994	A	S	S	T	I	H	N	K	T	K	R	D	N
	Modern lineage	JF912188/BeH622493/BRA/2000	A	S	N	T	I	H	N	K	T	R	R	D	D
	1D	JF912187/BeH622205/BRA/2000	A	S	N	T	I	H	N	K	T	R	R	D	D
		JF912189/BeAR646536/BRA/2001	A	S	N	T	I	H	N	K	T	R	P	V	D
		JF912190/BeH655417/BRA/2002	A	S	N	T	I	H	N	K	T	R	R	D	N
		KM388817/strain 2A/VEN/2004	A	S	N	T	I	H	N	K	T	R	R	D	N
		KM388814/strain6A/VEN/2005	A	S	N	T	I	H	N	K	I	R	R	D	N
		KM388818/strain8A/VEN/2006	A	S	N	K	I	L	S	N	T	R	R	D	S
		KM388815/strain 9A/VEN/2007	A	S	S	T	I	H	S	K	T	R	R	D	N
		KY861728/BeAn754036/BRA/2008	A	N	N	T	I	H	N	K	T	K	R	D	N
		KM388816/strain10A/VEN/2010	A	S	N	T	I	H	N	K	T	R	R	D	N
		KY885000/ES-504/BRA/2017	A	S	N	T	I	H	N	K	T	R	R	D	S
		KY885001/ES-505/BRA/2017	A	S	N	T	I	H	N	K	T	R	R	D	S
		MF423375/RJ87/BRA/2017	A	S	N	T	I	H	N	K	T	R	R	D	S
	1E	MF423376/RJ94/BRA/2017	A	S	N	T	I	H	N	K	T	R	R	D	S
		MF423377/RJ95/BRA/2017	A	S	N	T	V	H	N	K	T	R	R	D	S
		MF423378/RJ96/BRA/2017	A	S	N	T	V	H	N	K	T	R	R	D	S
		MF538785/RJ97/BRA/2017	A	S	N	T	V	H	N	K	T	R	R	D	S
		MF538786/RJ104/BRA/2017	A	S	N	T	I	H	N	K	T	R	R	D	S
		MF423373/PA193/BRA/2017	A	S	N	T	V	H	N	K	T	R	R	D	S
		MF423374/PA196/BRA/2017	A	S	N	T	I	H	N	K	T	R	R	D	S
		MF538782/H190/BRA/2017	A	S	N	T	I	H	N	K	T	R	R	D	S
		MF538783/H191/BRA/2017	A	S	N	T	V	H	N	K	T	R	R	D	S
		MF434851/H199/BRA/2017	S	S	N	T	I	H	N	K	T	R	R	D	S
		MF538784/H196/BRA/2017	A	S	N	T	I	H	N	K	T	R	R	D	S
	TT	HM582851/TVP11767/TTO/2009	A	S	N	T	I	H	N	K	T	K	R	D	N

		C			E				NS1	NS2A	NS3					NS5			
		25[d]	79[d]	86[d]	407[d]	409[d]	456[d]	547[d]	983[d]	1277[d]	1738[d]	1764[d]	1928[d]	2029[d]	2030[d]	2508[d]	2801[d]	3227[d]	3388[d]
West African YFV strains	AY640589/Asibi/GHA/1927	N	A	R	A	S	E	M	H	T	A	V	K	D	L	S	Y	Q	K
	JX898869/DakArAmt7/CIV/1973	N	A	R	A	S	E	M	H	V	A	I	K	D	L	R	Y	Q	K
	U54798/85-82H/CIV/1982	N	A	R	A	S	E	M	H	T	A	I	K	D	L	R	Y	Q	K
	JX898868/HD117294/SEN/1995	N	A	R	A	S	E	M	H	T	G	I	K	D	L	R	H	Q	K
	JX898871/ArD114896/SEN/1995	N	A	R	A	S	E	M	H	T	A	I	K	D	L	T	Y	Q	K
	JX898872/ArD114972/SEN/1995	N	A	R	A	S	E	M	H	T	A	I	K	D	L	T	Y	Q	K
	JX898870/ArD121040/SEN/1996	S	V	K	A	S	E	M	N	T	A	I	K	D	L	R	Y	Q	K
	AY603338/Ivory Coast/CIV/1999	N	A	R	A	S	E	M	H	T	A	I	K	D	Q	R	Y	H	K
	JX898873/ArD149214/SEN/2000	N	A	R	A	S	E	T	H	T	A	I	K	G	L	R	Y	Q	K
	JX898874/ArD149194/SEN/2000	N	A	R	A	S	E	M	H	T	A	I	K	D	L	R	Y	Q	K
	JX898875/ArD149815/SEN/2000	N	A	R	A	S	K	M	H	T	A	I	R	D	L	R	Y	Q	K
	AY572535/Gambia2001/GMB/2001	N	A	R	A	S	E	M	H	T	A	I	K	D	-	R	Y	H	K
	JX898876/ArD156468/SEN/2001	N	A	R	V	F	E	M	H	T	A	I	K	D	L	S	Y	Q	R
	JX898878/ArD181250/SEN/2005	N	V	R	A	S	E	M	H	T	A	I	K	D	L	R	Y	Q	K
	JX898879/ArD181676/SEN/2005	N	V	R	A	S	E	M	H	T	A	I	K	D	L	R	Y	Q	K
	JX898881/ArD181439/SEN/2005	N	V	R	A	S	E	M	H	T	A	I	K	D	L	R	Y	Q	K
	JX898877/ArD181464/SEN/2005	N	V	R	A	S	E	M	H	T	A	I	K	D	L	R	Y	Q	K
	JX898880/ArD181564/SEN/2005	N	V	R	A	S	E	M	H	T	A	I	K	D	L	R	Y	Q	K

South America genotype	Genbank accession number	Country	Isolation date
I	MF423373	Brazil	2017
	MF423378		
	MF538785		
	MF423377		
	MF538784		
	MF423374		
	KY885000		
	KY885001		
	MF423376		
	MF538783		
	MF434851		
	MF423375		
	MF538786		
	MF538782		
	KM388815	Venezuela	2007
	KM388818		2006
	KM388814		2005
	KM388816		2010
	KM388817		2004
	KY861728	Brazil	2008
	JF912190		2002
	JF912187		2000
	JF912188		2000
	JF912189		2001
	HM582851	Trinidad-Tobago	2009
	JF912185	Brazil	1992
	JF912182		1984
	JF912180		1981
	JF912184		1987
	JF912179		1980
	JF912186		1994
	JF912183		1984
II	KF907504	Bolivia	1999
	JF912181	Brazil	1983